THE ASTROPHYSICAL JOURNAL, 400:280–303, 1992 November 20

WHY STARS INFLATE TO AND DEFLATE FROM RED GIANT DIMENSIONS

ALVIO RENZINI, LAURA GREGGIO, AND CLAUDIO RITOSSA
Dipartimento di Astronomia, Università di Bologna, CP 596, I-40100 Bologna, Italy
AND
LILIA FERRARIO
Department of Mathematics, Australian National University, GPO Box 4, ACT 2601 Canberra, Australia
Received 1992 January 16; accepted 1992 May 28

ABSTRACT

We demonstrate that a unique physical process is responsible for the runaway expansion of stars to red giant dimensions, as well as for their subsequent recollapse leading to the formation of the so-called *blue loops*. In response to an increasing luminosity from the core, the stellar envelope expands keeping its thermal equilibrium insofar the envelope thermal conductivity increases. However, expansion implies local cooling, ion recombination, and thus increasing opacity, in such a way that a time comes when further expansion causes a drop of thermal conductivity in the envelope. As the luminosity transferred outwards and radiated away from the surface drops, thermal equilibrium is broken and an increasing fraction of the core luminosity is trapped in the envelope, causing further expansion and further drop of the thermal conductivity: the resulting runaway inflation of the envelope brings the star to the red giant region of the H-R diagram, and thermal equilibrium is not restored until convection penetrates inwards and the whole envelope becomes convective. The reverse process is responsible for the formation of the blue loops. During the early helium-burning phase, the core luminosity decreases and the star descends along the Hayashi track. By contraction the envelope heats up, the heavy ions ionize and the opacity drops. As the inner part of the envelope returns to radiative equilibrium, the envelope departs again from thermal equilibrium, since by contraction the temperature increases, the heavy ions ionize, the opacity drops, the thermal conductivity increases, and so do the radiative energy losses. Thus the envelope catastrophically deflates inside the gravitational potential well of the star. We present detailed analyses of these runaway inflations and deflations, and apply these concepts to achieve a deeper physical understanding of several major features of stellar evolution, including the pre–main-sequence phase, the overall contraction phase, and the formation of first and second blue loops. It is also recognized that the progenitor of the supernova 1987A was describing the so-called second blue loop, being far away from thermal equilibrium, when the explosion caught the star "on the fly" along such loop. The underlying physical mechanism responsible for the blue supergiant structure of the precursor is therefore identified. Finally, a general criterion for stellar thermal stability is formulated, and it is shown that when the criterion is violated either runaway inflations or deflations of the star are produced.

Subject headings: stars: interiors — stars: late-type

1. INTRODUCTION

Color-magnitude diagrams (CMD) of stellar populations show many stars near the main sequence (MS), many red giants, but very few stars at intermediate temperatures in what is known as the *Hertzsprung Gap*. Theoretical models for stars slightly more massive than the Sun, and near solar metallicity, shortly after their central hydrogen exhaustion experience a rapid expansion (from few $R_\odot$ to over 100 $R_\odot$) which on a thermal time scale brings them to the red giant region. Following their arrival on the Hayashi track, models reestablish their thermal equilibrium, and then the evolution proceeds on a nuclear time scale. We can say that there is excellent agreement between theory and observations, as models rapidly sweep across the H-R diagram right where only few stars are found: the Hertzsprung gap is nicely reproduced. While there is universal consensus on the simple statements above, opinions wildly diverge as to why models behave the way they do, or, in other words, as to *why stars become red giants.*

Quite a similar situation is encountered later in the evolution of the stars. During helium burning in the core, models can incur into a rapid contraction phase which—on a thermal time scale—brings them back to the *blue* region of the H-R diagram where they quietly burn their helium through central exhaustion. Again, the CMDs of star clusters and populations of the appropriate age show indeed many stars in the region that, by and large, is occupied by evolutionary models in the core helium burning phase which have experienced the mentioned rapid contraction, i.e., which are evolving along what is known as the *blue loop.*[1] Although the observed and theoretical morphology of the loops may occasionally differ in detail, also in this case we can say that there is universal consensus on the fact that theoretical evolutionary models exhibit a qualitative behavior which is in excellent agreement with the observations. Yet, opinions diverge again as to what is the physical origin of the loops, or, as to *why red giants deflate to blue giant dimensions*, during their core helium-burning phase.

Finally, models conclude their blue loops with a rapid expansion which is qualitatively very similar to that they have experienced earlier, and which brings them again to the red giant region. Yet, while rapidly expanding, models in an appropriate mass range may exhibit a temporary recontraction

[1] The blue loops during core helium burning are often called also *Cepheid loops*, as most Cepheid variable stars are in this evolutionary phase.

known as the *second blue loop* (to distinguish it from the *first* blue loop described above). In this case the loop is completed on a thermal time scale, which is too short for allowing any detailed comparison with observed CMDs. Although for this reason it is not possible to claim excellent agreement with CMD observations, a few Cepheids with exceptionally large rate of period change may be second blue loop objects. In any event, also the physical origin of the second blue loop remains to be understood.

The three questions above have been generally addressed separately one from another, in progressively more restricted circles of astronomers as complexities and technicalities increase when considering more and more advanced phases of evolution. There is only one exception, in which it has been claimed the solution to the three problems to be just one and the same, the common origin being in an opacity-driven thermal instability that affects stellar envelopes as they come to cross critical loci in the H-R diagram (Renzini 1984, hereafter Paper I; see also Iben & Renzini 1984). With few exceptions (Woosley, Pinto, & Ensman 1988a; Applegate 1988; Podsiadlowski, Joss, & Hsu 1992), the argument has been either rejected or criticized (Yahil & van den Horn 1985; Tayler 1988; Weiss 1989; Whitworth 1989; Bhaskar & Nigam 1991; Fujimoto & Iben 1991; Chiosi, Bertelli, & Bressan 1992), and other, completely different solutions have been proposed. In this paper we prove the correctness of all the arguments in Paper I, and expand them to identify and describe in full detail the physical origin of the expansion to red giant dimensions, as well as of the first and second blue loops. In doing so we encounter the still unsettled issue of the evolutionary history of the percursor of SN 1987A, and we take this opportunity for shedding fresh light on why it did happen to this object to explode as a blue supergiant, an event which had surprised many, even among stellar evolution practitioners.

In § 2 we present the theoretical background for our physical criterion for the occurrence of runaway inflations and deflations of stellar envelopes. This criterion is then illustrated by means of simplified numerical experiments which are presented, described and discussed in § 3. These experiments allow us to gather full understanding of the behavior of stellar envelopes under the action of predetermined stimuli coming from the stellar core. In § 4 we then apply the conceptual tools introduced in §§ 2 and 3 to the evolution of a 9 $M_\odot$ star with solar composition, for which we have computed the whole evolution from the main sequence to the asymptotic giant branch (AGB). In particular, the physical reasons for the envelope behavior during crucial evolutionary phases are identified and thoroughly discussed. Such phases include the pre–main-sequence phase, the overall contraction phase, the first inflation to red giant, and the first and second blue loops. The study of this particular evolutionary sequence then allows us to introduce a criterion for stellar stability which is of general validity. In § 5 we explain the physical origin of heretofore ill-understood evolutionary behaviors, such as the sensitivity of blue loops to many fine details of the input physics, and we then continue discussing the origin of the mass and composition dependence of the morphology of evolutionary tracks. As an application of these conceptual tools we briefly discuss the case of the precursor of SN 1987A, clarifying the evolutionary connections which lead to a blue supergiant exploder. In § 6 we present a brief discussion comparing our criterion for inflation/deflation to other criteria that we believe are invalid. Our main conclusions are summarized in § 7.

2. THEORY OF THE ENVELOPE THERMAL INSTABILITY

The evolution of stars is driven by two main factors: energy losses through the surface and nuclear transmutations in the interior. When the total rate of nuclear energy generation (L_N) equals the surface luminosity (L_S), the star is said to be in *thermal equilibrium*.[2] Stars are in thermal equilibrium (TE) through most of their lives, but they depart from TE during crucial evolutionary phases which correspond to either the final consumption or ignition of a nuclear fuel in the core, or to the development of a thermal instability in the envelope. The discussion of the origin, physical properties, and implications of this latter type of events is the main topic of this paper. The guideline of our reasoning is rather obvious indeed: when more energy is generated than is radiated away ($L_N > L_S$) the structure expands, and vice versa, it contracts when its energy losses are not compensated by the nuclear sources ($L_N < L_S$). Still, if by such expansion/contraction $|L_N - L_S|$ decreases, then TE can be maintained and/or approached. When instead $|L_N - L_S|$ increases the structure can precipitously depart from TE, setting into either a runaway expansion or a runaway contraction, depending on the sign of $L_N - L_S$.

Before proceeding further, we state a few clear definitions in order to avoid semantic misunderstandings. By stellar *core* we mean the inner part of the star which has been affected by appreciable hydrogen nuclear burning; by *envelope* we mean the outer part of the star which is still unburned. Also, for nonpractitioners it is worth recalling the different role played by the energy generation and radiative energy transfer equations of stellar structure:

$$\frac{dL_r}{dM_r} = \epsilon_n + \epsilon_g \tag{1}$$

$$L_r = -4\pi r^2 \frac{4acT^3}{3\kappa\rho}\frac{dT}{dr} = 4\pi r^2 F_{\rm rad}\,, \tag{2}$$

where neutrino losses are ignored. Equation (2) dictates that the luminosity L_r transmitted by a generic layer in radiative equilibrium is always given by the product of the surface area times the local radiative flux $F_{\rm rad}(r)$, no matter whether nuclear burning is active or not, or is sufficient to balance the energy transfer. Equation (1), instead, dictates that when for any reason $dL_r/dM_r \neq \epsilon_n$, then $\epsilon_g \neq 0$, TE is broken, and rapid expansion or contraction has to set in.

During most of the core hydrogen-burning phase, the stellar core contracts as a consequence of the increasing molecular weight, and becomes more luminous primarily as a consequence of the decreased opacity (for a classical description of this evolutionary phase see Iben 1965b). Clearly, both trends result mainly from the decreased number of electrons per unit mass, as hydrogen is gradually transformed into helium. No such transformations take place in the envelope, which then *follows* the evolution of the core, i.e., it is forced to readjust itself to the changing structure of the core, on top of which it sits, and from which it receives the energy flux. Again, during most of the core hydrogen-burning phase the (energetic) effect of the increasing core luminosity overwhelms the (mechanical) effect of the decreasing core radius, so the envelope has mainly to react to the increasing luminosity which is impinging at its

[2] Strictly speaking thermal equilibrium requires that the coefficient of *gravitational energy generation* ϵ_g is negligible throughout the whole structure, i.e., $\int |\epsilon_g| dM_r \ll L_S$.

base, and that has somehow to be transferred outwards and radiated away.[3] To understand the reaction of the envelope we proceed with a simple *gedankenexperiment*: we start with the envelope structure in TE ($L_r \simeq L_B \simeq L_S$, L_B being the luminosity at the base of the envelope, i.e., the core luminosity). We now suppose to slowly increase L_B so as to simulate the secularly increasing luminosity of the core, while the envelope density and temperature distributions are kept the same. Since the transmitted luminosity—determined by equation (2)—remains the same, more energy enters the envelope at its base than leaves it from the surface ($L_S < L_B$), and thermal energy is correspondingly trapped in the envelope. Heat trapping causes temperature increase, excess pressure, and then hydrostatic imbalance. In turn, the excess pressure causes expansion which allows the hydrostatic equilibrium of the envelope to be restored. This is indeed the way stellar models behave, and while the envelope expands, the surface area $4\pi r^2$ increases (trivial), and the radiative flux drops, but their product—the transmitted luminosity—can either increase or decrease, depending on the details of the local evolutionary transformation. The two possible behaviors have dramatically different consequences. In the former case the increase in the transmitted luminosity allows to keep near equality between the core luminosity and the luminosity transmitted outwards through the envelope and radiated away from the surface: i.e., L_S adjusts to L_B and TE can be maintained, as during the main-sequence phase. In the latter case, when expansion implies a decrease in the transmitted luminosity, then thermal energy is trapped in the envelope and causes further expansion, which in turn produces a further decrease in the transmitted luminosity: the result is a runaway expansion of the envelope which increasingly diverges from TE, i.e., L_S drops precipitously, thermal energy is trapped in the envelope at an increasing rate $L_B - L_S$, and this energy is used to drive a catastrophic expansion of the envelope. In Paper I it has been argued that this is the reason why stars become red giants, and in this paper we prove the assertion, by elucidating the physical origin of the instability, and by showing with the help of numerical experiments and full evolutionary models how the instability sets in, develops, and what are its evolutionary consequences.

To investigate the nature of the runaway, we need to look in more detail to how the transmitted luminosity is affected by local variations of radius, i.e., by local expansions (or contractions). To this end we start from equation (2), and express the temperature gradient in terms of the so-called effective polytropic index n (see Schwarzschild 1958):

$$n + 1 = \nabla^{-1} = \frac{d \ln P}{d \ln T} = \frac{\mu H \beta_g}{k} \frac{GM_r}{r^2} \left(- \frac{dT}{dr} \right)^{-1} , \quad (3)$$

or,

$$- \frac{dT}{dr} = \frac{\mu H \beta_g}{k} \frac{GM_r}{r^2} \frac{1}{n+1} , \quad (4)$$

where we have used the equation of hydrostatic equilibrium, all the symbols have the usual meaning, and $\beta_g = P_G/P$ is the ratio of the gas to total pressure. Substituting equation (4) into equation (2) we finally get

$$L_r = \frac{4\pi \mu H \beta_g GM_r}{k} \frac{4acT^3}{3\kappa\rho} (n+1)^{-1} . \quad (5)$$

Since the polytropic index does not change much, what matters most is the behavior of the quantity $K = 4acT^3/3\kappa\rho$, which is the local thermal conductivity for layers in radiative equilibrium. If during expansion the thermal conductivity increases then near TE can be maintained; if it decreases the energy flux gets increasingly trapped in the envelope, and a runaway expansion sets in. Correspondingly, the question "*why stars become red giants?*" is equivalent to ask "*why in the course of post–main-sequence evolution the envelope thermal conductivity first increases, and then decreases?*"

We denote with $\delta X(M_r)$ the *evolutionary* variation of the generic quantity X at the mass coordinate M_r, i.e., the variation of $X(M_r)$ between two *consecutive* configurations of the star (such as between two consecutive stellar models). Conversely, by $dX(M_r)$ we mean the difference of $X(M_r)$ between two *adjacent* mass points, i.e., the radial differential of X at one given time. We now concentrate on one specific mass coordinate M_r, and follow the evolutionary variation $\delta \ln L_r$ of the transmitted luminosity, resulting from an evolutionary expansion $\delta \ln r$. Thus, taking the natural logarithm of equation (5), assuming both μ and β_g to be constant in time, and differentiating, one gets

$$\delta \ln L_r = (3 + \beta) \delta \ln T - (1 + \alpha) \delta \ln \rho - \delta \ln (n+1) , \quad (6)$$

or, equivalently,

$$W(M_r) = \frac{\delta \ln L_r}{\delta \ln r} = -(3 + \beta) A - (1 + \alpha) \frac{\delta \ln \rho}{\delta \ln r} - \frac{\delta \ln (n+1)}{\delta \ln r} , \quad (7)$$

where $\alpha = (\partial \ln \kappa / \partial \ln \rho)$, $\beta = -(\partial \ln \kappa / \partial \ln T)$, and $A = -\delta \ln T / \delta \ln r$. Imposing mass conservation, and assuming that the transformation is locally quasi-homologous (i.e., if $d\delta \ln \rho \simeq d\delta \ln T \simeq 0$), it can be shown that

$$\frac{\delta \ln \rho}{\delta \ln r} \simeq A - 4 , \quad (8)$$

to first order in the evolutionary changes. Under the same assumptions the polytropic index remains the same in the course of the evolutionary change—i.e., $\delta \ln (n+1) \simeq 0$—and inserting equation (8) into equation (7) we derive

$$W(M_r) \simeq 4(1 - A) + (4 - A)\alpha - A\beta , \quad (9)$$

which is the approximate relation for the W function given in Paper I.[4] Now, neither the polytropic index and β_g are strictly constant in the course of the evolution, nor strictly homologous are the local temperature and density variations. In particular, when the core contracts and the envelope expands there is a macroscopic departure from the homology relations, A and W have poles at the stagnation point where $\delta \ln r = 0$ and where even the sign of W in equation (7) and in equation (9) can be different. We therefore do not expect equation (9) to give a very accurate representation of the true W where A

[3] There is a relatively brief phase just before central hydrogen exhaustion (the so-called overall contraction phase) during which the effect of core contraction overwhelms that of the increasing luminosity. This will be discussed in detail in § 5.2.

[4] Note that if the evolutionary change is strictly homologous then $A = 1$, and therefore $L \propto R^{3\alpha - \beta}$, see Jeans (1925, 1928).

departs significantly from unity, in particular when approaching the stagnation point where $A \to \infty$. Still, out in the envelope, away from the stagnation point the main physics of the problem is retained when passing from the exact equation (7) to the approximate equation (9), and indeed we have verified that there equation (9) provides a fair approximation. In any event, both equations (7) and (9) are here used just to grasp the physical nature of the thermal instability leading to the runaway expansion of the envelope.

If the polytropic index does not evolve with time (which is true to a fairly good approximation) the function $W(M_r)$ reduces to the evolutionary derivative of the thermal conductivity. Thus, from either equation (7) or equation (9) it is apparent that the density and temperature derivatives of the opacity play a crucial role in determining the behavior and the sign of the function W. Correspondingly, we can anticipate that in real stars the particular behavior of the radiative opacity bears the prime responsibility as to why stars become red giants. Indeed, during the main-sequence phase most of the envelope is at fairly high temperatures ($T \gtrsim 5 \times 10^6$ K), matter is fully ionized, electron scattering dominates the opacity, and the opacity derivatives α and β are vanishingly small. However, as the star expands, an increasing fraction of its envelope cools below $\sim 5 \times 10^6$ K, the heavy metals (Fe, Si, Ar, Mg, Ne, ... and eventually also O, N, and C) start partly to recombine in their K levels, the opacity increases because of the bound-bound and bound-free transitions now becoming available, and α and β approach their Kramers' values, 1 and 3.5, respectively. Eventually, in the envelope the thermal conductivity and the transmitted luminosity reach a maximum and then decrease, the function W becomes negative, and the expansion develops into a runaway which brings the star to the red giant region. "Ultimately, the thermal instability can be described as a runaway partial recombination of the heavy ions in the envelope" (Paper I).

Following the arguments in Paper I, we now state that the condition

$$W(M_r) > 0 \tag{10}$$

holding through the whole envelope is a sufficient condition for a stellar envelope to be able to adjust itself to the core luminosity, and therefore approach and maintain a TE configuration. Conversely,

$$W(M_r) < 0 \tag{11}$$

is a necessary condition for a thermal instability to set in in the envelope.[5] As anticipated in Paper I, the appearance of a negative W in the stellar envelope can lead to either a runaway expansion, or to a runaway contraction, depending on the particular evolutionary phase at which the change in the sign of W takes place. The runaway envelope expansion takes place when L_B increases, but the ability of the envelope to transfer energy outwards (i.e., its thermal conductivity) decreases. Seemingly, a runaway envelope contraction (a *star slide*) takes place when L_B decreases, the envelope shrinks, but its transparency to radiation increases, i.e., L_S increases. Now the envelope is losing more energy than it receives from the core, and therefore it is forced to contract. Yet, as the envelope contracts its thermal conductivity further increases, its energy losses amplify, and it catastrophically deflates. This is indeed the origin of the famous blue loops during the helium-burning phase, which are then due to the same kind of thermal instability leading to red giant formation, now working in the reverse direction. Ultimately, the loop formation can be described as a runaway ionization of the heavy metals in the envelope. In summary, the runaway expansion to red giant dimensions begins when a maximum is reached in the envelope thermal conductivity, and the runaway contraction from the red giant branch begins when the thermal conductivity reaches a minimum. This assertion will now be illustrated with quantitative examples.

[5] These statements apply to the envelope, and as such they are not immediately extendable to the stellar core. For example, during most of the core hydrogen-burning phase the core contracts and gets more luminous (i.e., $W < 0$), yet the core is in TE. We shall return to this point in § 4.7.

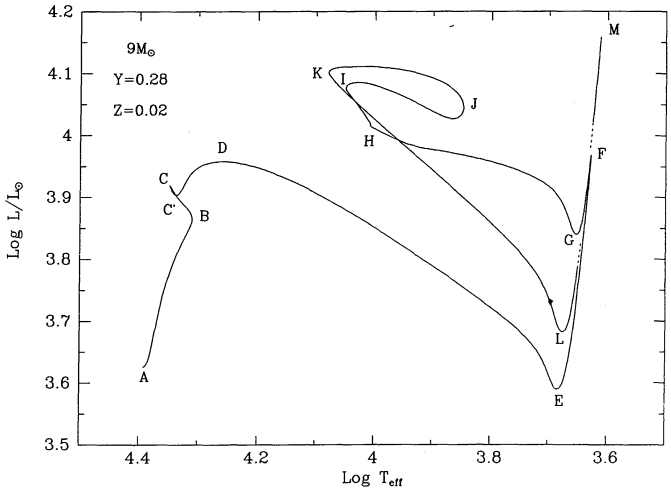

FIG. 1.—Evolution in the H-R diagram of a 9 $M_\odot$ model of solar composition. The letters identify crucial evolutionary points which are discussed in the text.

3. NUMERICAL EXPERIMENTS WITH TOY ENVELOPES

The theoretical tools developed in the previous section are now put at work on detailed examples of runaway envelope expansions and contractions, where the behaviors of opacity, thermal conductivity, the W-function, and then stellar radius are organized in the proper causal sequence. For this purpose we have first computed the evolution of a 9 $M_\odot$ star of solar composition $(Y, Z) = (0.28, 0.02)$, from the zero-age main sequence all the way to the early AGB phase. The evolutionary sequence has been computed using the code FUJIMO kindly provided to us by Icko Iben Jr. The code has been partly vectorized to run on a Cray computer. Figure 1 shows the corresponding evolutionary track in the H-R diagram, while the evolutionary age at several relevant points along the sequence is given in Table 1. This sequence will be discussed in

TABLE 1

EVOLUTIONARY TIMES FOR THE 9 $M_\odot$ SEQUENCE

Point	Time (10^6 yr)	Point	Time (10^6 yr)
A	0.0000	G	24.3046
B	21.8130	H	24.8211
C	22.5220	I	26.1765
C'	22.5378	J	26.7813
D	22.6435	K	26.8740
E	22.7752	L	26.9380
F	22.8126	M	26.9488

detail in the next section, while here we present the result of numerical experiments which are limited to the stellar envelope of this 9 $M_\odot$ model.

The occasional complications of the behaviors of the models through crucial evolutionary phases is at least in part responsible for the long delay with which the physical origin of the expansion to red giant dimension has been understood. To avoid such complexities we have constructed sequences of evolutionary models restricted to the homogeneous envelope, so as to isolate the direct cause of the envelope expansion. For this purpose, we have replaced the usual central boundary conditions ($r = 0$ and $L_r = 0$ for $M_r = 0$) with a new set of boundary conditions at the base of the envelope: $r = R_B$ and $L_r = L_B(t)$ for $M_r = M_B$, with M_B and R_B being, respectively, the mass and the radius of the stellar core. In doing so we do not bother about the detailed structure of the core, but just follow the reactions of the envelope to changes of the core luminosity, that we are free to vary at our leisure. For this purpose the Henyey code works as well for the lonely envelope as it usually does for the entire structure.

For the experiment we have assumed $R_B = 0.63\ R_\odot$ and $M_B = 2\ M_\odot$, appropriate to the corresponding full model when it is near the exhaustion of hydrogen at the center. For the initial core luminosity we have adopted $L_B = 7450\ L_\odot$ which also corresponds to a full model close to central hydrogen exhaustion. After having constructed a static envelope model (with $\epsilon_g = 0$, and therefore $L_S = L_B$), we have allowed the bottom luminosity to increase linearly with time, reaching 11,700 $L_\odot$ in 10^6 yr, which corresponds to the luminosity at the central helium ignition in the full model (see Fig. 1). The time taken by the full model to evolve from central hydrogen exhaustion to central helium ignition at the tip of the red giant branch is somewhat shorter, about 3.4×10^5 yr. Past the maximum, L_B has been linearly decreased back to 7450 $L_\odot$ in another 10^6 yr, so as to mimic the effects of the luminosity decrease that the whole star would experience past helium ignition in the core. It is worth stressing that during the whole experiment the core radius and mass are kept strictly constant.

A somewhat similar experiment was conducted by Woosley et al. (1988a) in relation to the evolution of the progenitor of SN 1987A (see § 5.4). One crucial difference however, exists in that Woosley et al. constructed a series of TE models for various values of the bottom luminosity L_B, while in the present experiment TE is *not* a priori enforced, but the envelope is left free to either approach to, or depart from TE under the influence of the varying L_B and of its own reactivity, i.e., ϵ_g is allowed to assume the values which are appropriate to the evolving configuration of the envelope.

As a reaction to the varying luminosity at its base, the envelope undergoes an extended excursion in the H-R diagram, which is shown in Figure 2. Several close analogies with the evolution of the complete model in Figure 1 are immediately apparent. In response to the increasing L_B, the envelope expands, and the surface luminosity initially increases. However, as the envelope cools the heavy ions progressively recombine, opacity increases, and the increase in thermal conductivity slows down until a maximum is reached (point B). Past this maximum, both thermal conductivity and surface luminosity drop, and the increasing power $L_B - L_S$ is trapped in the envelope, and used to *lift* envelope material inside the potential well of the star. The runaway expansion brings the envelope to lower and lower temperatures, higher and higher opacities, until an enlarging convective zone appears, first near the surface, and eventually the whole envelope turns convective. As convectivization proceeds, energy transfer is not described any more by equation (2) which applies to radiative equilibrium, and the thermal instability damps out: the envelope has reached the Hayashi track (point C). Shortly after the arrival on the Hayashi track TE is effectively restored through the envelope, and the model climbs along the Hayashi track, up to the imposed tip luminosity (point D). Subsequently, as the luminosity at the base of the envelope starts decreasing, the model traces back its previous evolution along the Hayashi line, and as the envelope contracts, temperature increases, opacity decreases, the radiative gradient decreases and a radiative zone appears and grows at the base of the envelope. Shortly after its appearance, the radiative zone becomes thermally unstable, i.e., W becomes negative in the contracting envelope, thermal conductivity starts increasing and so does the transmitted luminosity (point E). Since now $L_S > L_B$, energy losses force the envelope to contract more rapidly, but the more rapidly it contracts the more energy is lost and a runaway deflation finally brings the envelope back to its original configuration, and TE is restored as L_S approaches L_B.

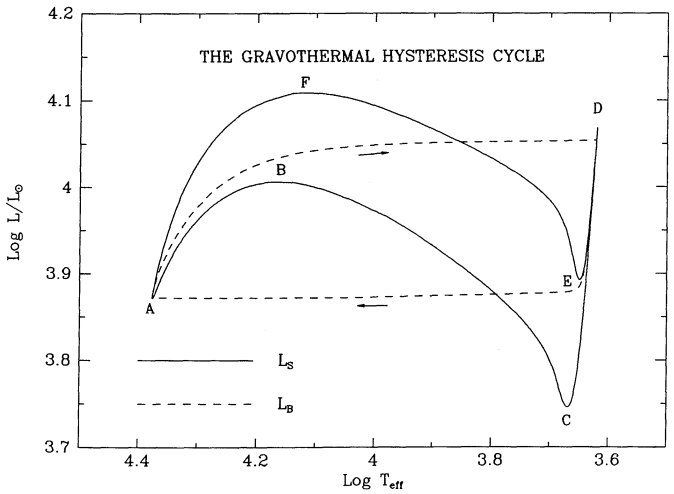

FIG. 2.—Gravothermal hysteresis cycle of the envelope in the H-R diagram, showing the variation of surface luminosity L_S and effective temperature under the action of a varying luminosity at the base of the envelope (L_B).

We define *gravothermal hysteresis cycle* (GTHC) the closed loop described by the envelope in Figure 2. During the runaway expansion thermal energy of the envelope is converted into gravitational potential energy, which—during the subsequent recollapse—is partly transformed back to thermal energy. Note that during the envelope inflation the absorption of radiative energy (at a rate $L_B - L_S$) assists the expansion, while during envelope deflation part of the gravitational energy is radiated away (at a rate $L_S - L_B$), as follows from the virial theorem. Actually, we have verified that during both inflation and deflation the virial theorem is fulfilled *locally* with a very good approximation (local quasi-viriality), i.e., "*one-half of the energy required to maintain local expansion is taken from the local thermal energy and one-half is abstracted from the local energy flow*" (Iben 1965b), and vice versa during deflation. The analogy with other hysteresis physical phenomena is evident, such as the fact that for a range of luminosities there exist two thermally stable envelope configurations, one radiative and the other convective, and which of the two is chosen by the star depends on the previous history of the envelope. Under these

circumstances the equations of stellar structure admit multiple solutions, thus violating the Vogt-Russell theorem (see also Kähler 1978; Kippenhahn & Weigert 1989). It must be noticed, however, that from a mathematical point of view the reference to multiple solutions of the equations is improper, as one of the four differential equations is different when either radiative or convective energy transfer is assumed. Uniqueness remains in the sense that there is only one TE radiative configuration, and only one TE convective configuration.

Figure 3 further illustrates the case. It shows the variations of L_B and L_S through the whole cycle from the initial configuration, to the red giant tip, and back to the initial state. As L_B starts increasing the envelope first reacts with a tiny decrease in surface luminosity caused by energy absorption in the envelope itself as it starts expanding. Then L_S follows the increase of L_B, though a sizable difference remains, and strict TE is approached but not reached. This moderate departure from TE is a result of the rather rapid increase in L_B that we have adopted, as demonstrated by the following example. In the experiment shown in Figure 4 the bottom luminosity is increased between the same limits as in Figure 3, but with a 20 times slower rate. The result is that initially L_S is now very close to L_B, and TE is very closely maintained. The amount of work needed to lift the envelope by a given extent inside the potential well being fixed, clearly the slower the expansion, the smaller the fraction of the available power L_B that is required for the lift. As far as W remains positive no major departure from TE is encountered. But, due mainly to the secular

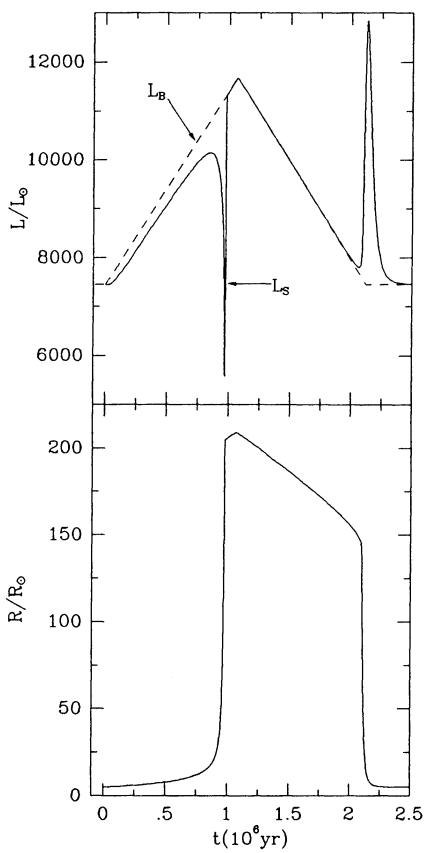

FIG. 3.—*Upper panel*: the time evolution of the output surface luminosity (*solid line*) in response to the imposed variation of the input luminosity at the base of the envelope (*dotted line*), for the whole gravothermal hysteresis cycle. The corresponding evolution of the radius is shown in the lower panel.

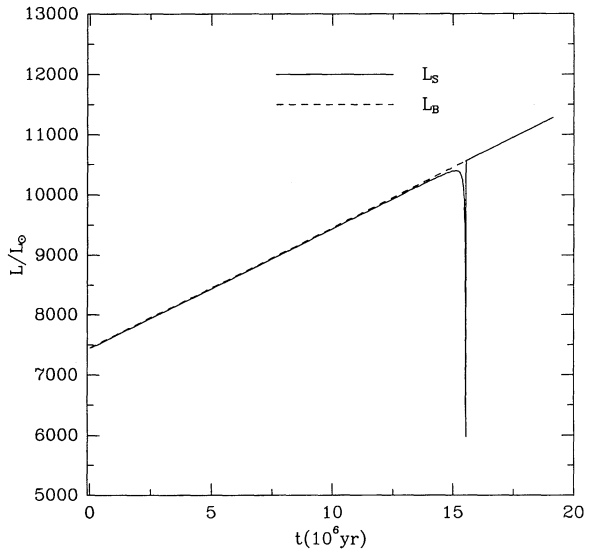

FIG. 4.—Time evolution of the input and output luminosity L_B and L_S as in Fig. 3, but for a 20 times slower increase in the input luminosity.

increase of β, the function W decreases at every point with time, and its inverse W^{-1}—which can be interpreted as the *reactivity* of the radius to variations of luminosity, see Paper I—tends to diverge. As W vanishes the thermal instability breaks out, L_S begins to drop, and the power absorbed in the envelope (i.e., $L_B - L_S$) dramatically increases. Correspondingly, the rate of expansion accelerates as shown by the lower panel in Figure 3, until the envelope turns convective, W returns to positive values and almost strict TE is quickly restored. During the subsequent contraction along the Hayashi line, TE is initially maintained with a very good approximation, until the inner part of the envelope turns radiative and soon becomes thermally unstable. Then $L_S - L_B$ dramatically increases and the envelope collapses inside the potential well of the star. It is crucial to realize that the occurrence of the runaway inflation and deflation is unavoidable, no matter how slowly the luminosity L_B is increased or decreased between its two limits.

As a general rule, when TE is broken models evolve on a thermal time scale, and the runaway expansion and contraction during the GTHC are no exception. Thus, it takes of the order of one Kelvin-Helmholtz time for the envelope to flip from the radiative to the convective configuration; the *inertia* of the envelope prevents an instantaneous jump from one to the other thermally stable configuration. In particular, in the *fast* experiment shown in Figure 3 the envelope takes $\sim 1.5 \times 10^5$ yr to evolve for the onset of the instability—the first relative maximum of L_S, when W first becomes negative—to the reestablishment of TE on the Hayashi line—when W returns to positive values. In the case of the *slow* experiment shown in Figure 4 the transition is appreciably slower, i.e., $\sim 4 \times 10^5$ yr.

To further familiarize with the GTHC, Figures 5 and 6 display the cycle in the input-output luminosity plane ($L_B - L_S$), and in the $L_B - R$ plane, respectively, R being the surface radius. The figures are self-explanatory. Figure 7 shows the evolution through the whole GTHC of the local thermal conductivity as a function of the local temperature, for the mass coordinate $M_r = 6\ M_\odot$, that we have chosen as representative of a generic mass point inside the envelope. Of course, quite similar loops in the $K-T$ plane are described by any

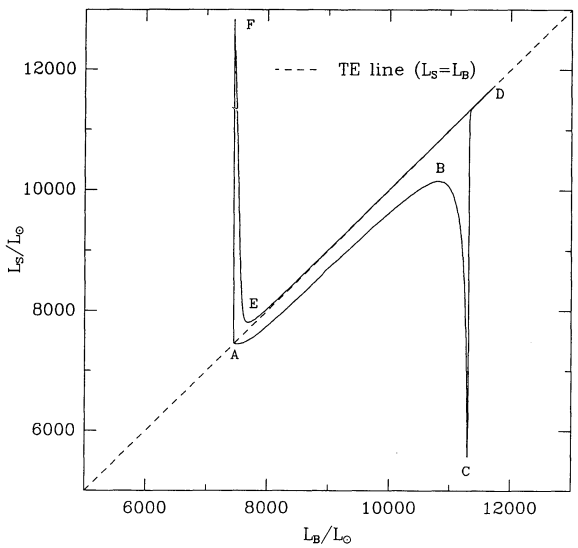

FIG. 5.—Gravothermal hysteresis cycle in the $L_B - L_S$ plane. The letters identify the same evolutionary points as in Fig. 2.

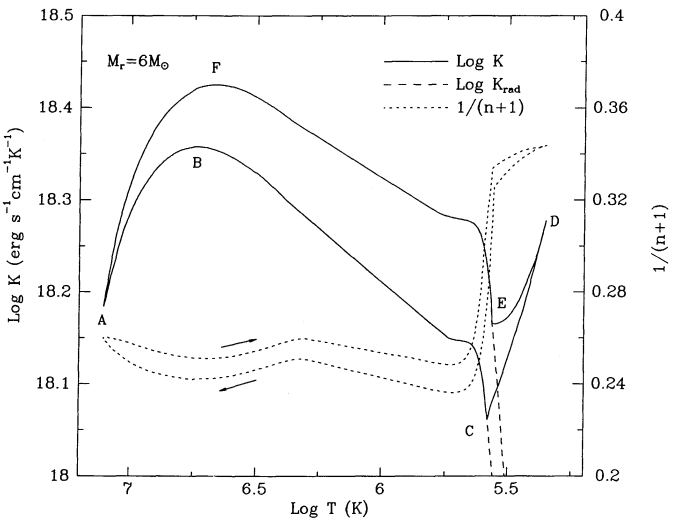

FIG. 7.—Thermal conductivity K vs. temperature at $M_r = 6\ M_\odot$ through the gravothermal hysteresis cycle. Also shown is the corresponding run of $(n + 1)^{-1}$, where n is the polytropic index. The letters identify the same evolutionary points as in Fig. 2.

other mass point in the envelope. Here $K = K_{rad}$ or $K = K_{conv}$, depending on whether the $M_r = 6\ M_\odot$ mesh point is radiative or convective, the convective conductivity being

$$K_{conv} = \frac{k}{4\pi\mu H\beta_g GM_r}\frac{L_r}{\nabla}, \qquad (12)$$

where, $\nabla\ [\equiv (n + 1)^{-1}] \simeq \nabla_{ad}$ in the deep interior where convection is nearly adiabatic. The similarity of Figure 7 to Figure 2 is not casual: thanks to equations (5) and (12) the luminosity is basically proportional to the thermal conductivity, while the polytropic index plays just a marginal role, being fairly constant during most of the cycle, apart from the quick transitions from radiative to convective equilibrium and vice versa. Therefore, it becomes immediately apparent that *the loop in the H-R diagram is nothing else but the outermost of the series of similar loops described by each mass shell in the K − T diagram.* The heat-proof inhabitants of stellar depths would hardly trust their theoreticians telling them that the evolution of their environmental conditions K and T would be perceived by hypothetical aliens of the outer space as something called the *Color-Magnitude Diagram*! Yet, this is the way it is. The case will be further commented in § 4 (see in particular Fig. 13).

Figure 7 also shows the evolution of the polytropic index, which remains nearly constant ($n \simeq 3$, appropriate for radiative equilibrium) through the whole runaway expansion, and starts decreasing only when the considered mesh point is about to become convective, i.e., when the envelope is already very close to the Hayashi line. Later, when the mesh becomes convective, the polytropic index returns to be nearly constant ($n \simeq 1.5$, as expected for a region in near adiabatic equilibrium). Figure 7 plainly demonstrates (opposite to what was claimed by Eggleton & Faulkner 1981 and Bhaskar & Nigam 1991) that (1) the variation of the polytropic index is a consequence, not a cause of stars becoming red giants, (2) that n never grows beyond ~ 3, and (3) that when the star is actually a red giant it decreases to ~ 1.5, instead of increasing towards ~ 5.

Figure 8 shows the behavior of the function $W(M_r)$ through the first breaking of thermal stability, i.e., around the first relative maximum of L_S. It is worth emphasizing that $W(M_r)$ first vanishes near the surface, and then its zero rapidly moves inward until $W < 0$ in the whole envelope. This further demonstrates that the thermal instability is a mere envelope phenomenon, which originates in the outer (i.e., cooler and more opaque) part of the envelope, and then rapidly propagates towards the interior. The behavior of the opacity and its derivative β is displayed in Figure 9, showing how dramatically these quantities increase through the runaway inflation of the envelope. Of course, all these variations are due to the strong cooling of the envelope during inflation, which is illustrated in Figure 7 and further in Figure 9. The run of the polytropic index across the envelope, for the same models before and after the breaking of TE is also displayed in Figure 9. Altogether, these figures clarify the relative role of the various quantities in

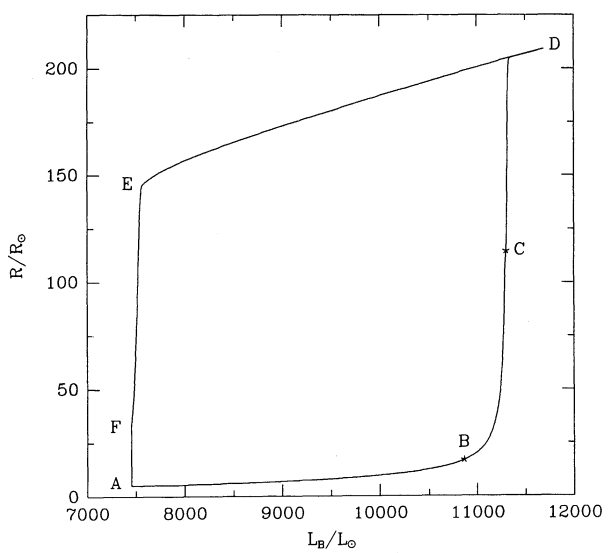

FIG. 6.—Gravothermal hysteresis cycle in the $L_B - R$ plane. The letters identify the same evolutionary points as in Fig. 2.

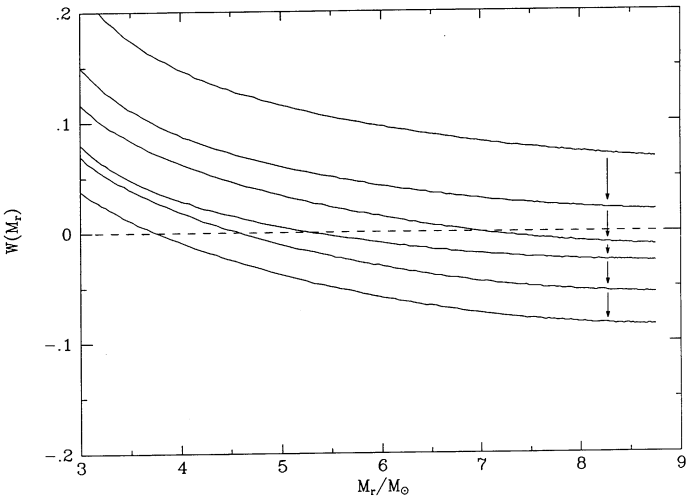

FIG. 8.—Function $W(M_r)$ at six representative times across the runaway expansion (from before to well after point B in Fig. 2). The first (uppermost) line refers to $t = 7.995 \times 10^5$ yr since the beginning of the experiment, and the subsequent configurations correspond to successive time intervals of 3.5×10^4, 1.7×10^4, 1.4×10^4, 9.6×10^3, and 1.4×10^4 yr, respectively, in the sequence indicated by the arrows.

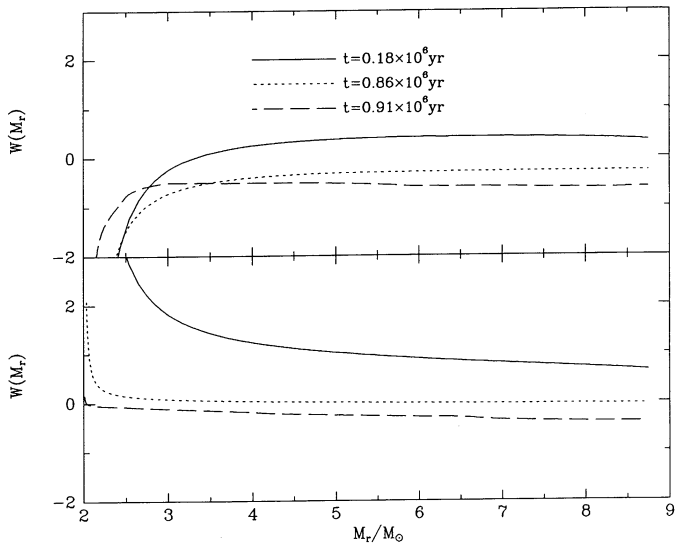

FIG. 10.—Function $W(M_r)$ as computed from eq. (9) in the upper panel, and as obtained from the exact relation (7) in the lower panel, for the same epochs of Fig. 9.

determining the change of sign in W, and then the onset of the instability.

In Figure 10 the run of $W(M_r)$ as computed from the approximate equation (9)—in the upper panel—is compared to the exact W shown in the lower panel. The comparison reveals that the approximate relation reproduces the gross features of the exact one for sufficiently large values of M_r, but may appreciably differ in detail, as anticipated when we have introduced it, and as protested by Weiss (1989). Yet, to understand the physical origin of the thermal instability, the approximate relation is as good as the exact one, and just in this mood it was introduced in Paper I.

Figure 11 now shows the true W's through the first red giant minimum (RGM), i.e., the minimum luminosity at the foot of the Hayashi line, when TE is restored. We note that $W(M_r)$ first becomes positive in the outer part of the envelope which has turned convective, and then the region of positive $W(M_r)$ expands towards the interior, with the zero being always in the radiative region, just below the base of the convective zone. It is indeed the increase in ∇_{rad} (decrease in n) which eventually

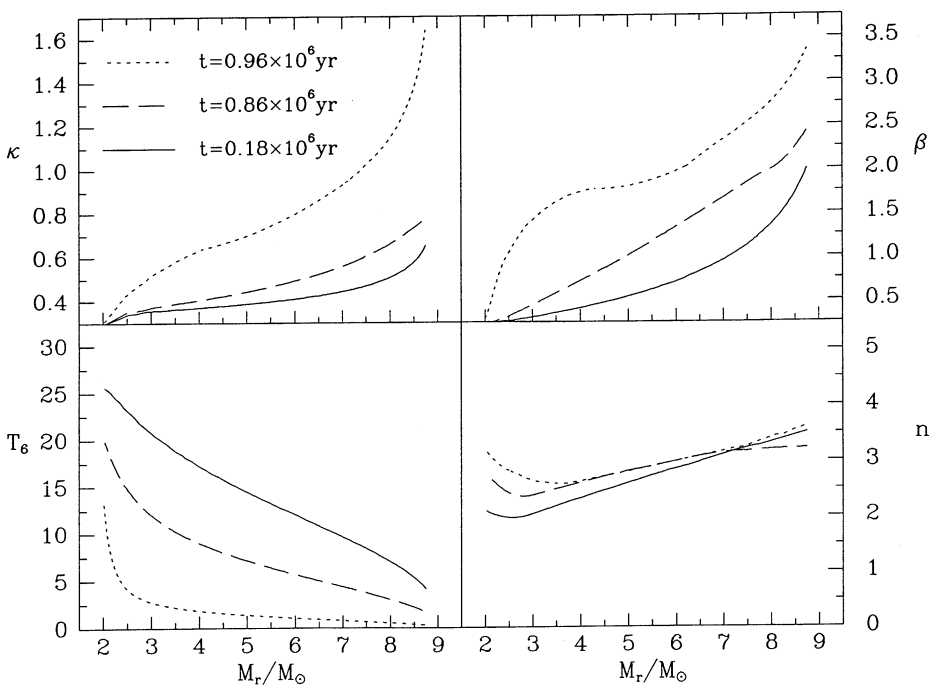

FIG. 9.—Opacity κ, its derivative β, the temperature in million K units T_6, and the polytropic index n for three envelope models through the runaway expansion. The times are indicated in the upper left panel.

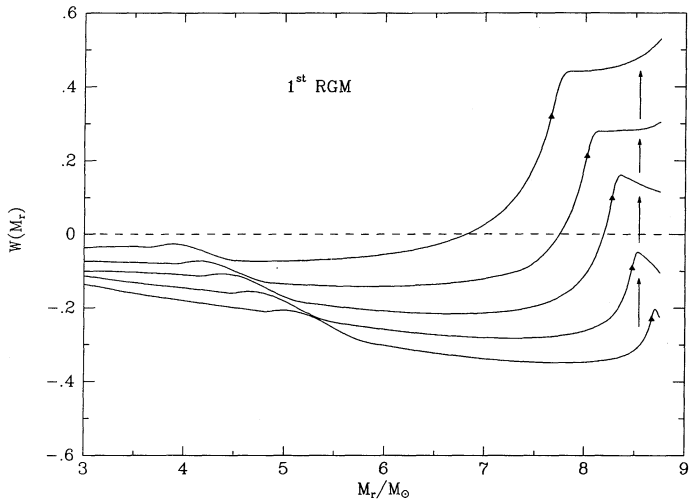

FIG. 11.—Function $W(M_r)$ for several models through the first red giant minimum. The filled triangle marks the mass location of the base of the convective envelope for each of the displayed models. Across the first red giant minimum $W(M_r)$ increases with time, so the earlier model is represented by the bottom line, and the latest shown model by the top line. The wake between 4 and 5 $M_\odot$ is an artifact of the opacity algorithm.

causes the local luminosity to start increasing again: if any, the role of changing polytropic index is to modestly anticipate the return to TE.

Figure 12 shows the behavior of the true W's through the second RGM, which marks the start of the runway contraction of the envelope. We see that the point which first becomes unstable ($W < 0$, $\delta \ln L_r > 0$), nearly coincides with the base of the convective envelope. Note that here the W's exhibit the reverse behavior with respect to the first RGM. In particular, the instability does not appear immediately as the base of the envelope becomes radiative, because the increase in the radiative thermal conductivity in equation (5) is initially overrun by the increase of the polytropic index, which rapidly jumps from ~ 1.5 to ~ 3. Again, we see that the change of polytropic

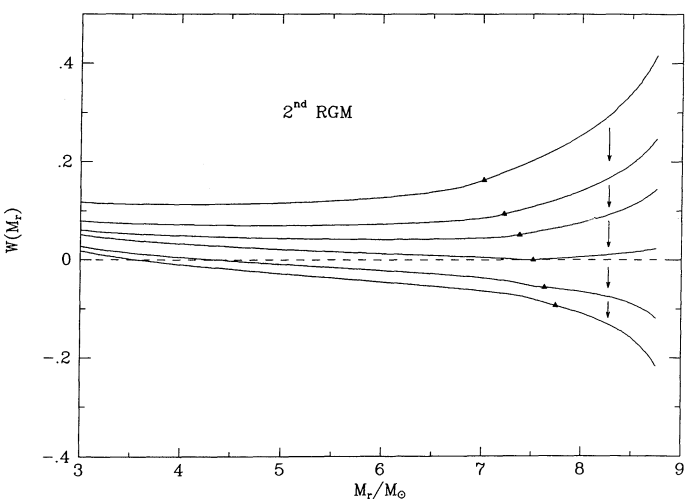

FIG. 12.—Function $W(M_r)$ for several models through the second red giant minimum. The filled triangle marks the mass location of the base of the convective envelope for each of the displayed models. Across the second red giant minimum $W(M_r)$ decreases with time, so the earlier model is represented by the top line, and the latest shown model by the bottom line.

index actually delays the onset of the thermal runaway, while its increase accompanies (without causing it) a catastrophic deflation (not expansion!) of the envelope. It is somewhat astonishing to realize to what extent the role of the polytropic index was misunderstood (see ref. above). In passing, we also note that similarly misunderstood was the role of the core-envelope jump in mean molecular weight. In this numerical experiment the envelope inflates and deflates, and yet μ is strictly constant through the structure during the whole GTHC.

During inflation L_r decreases outwards in the envelope as energy is being absorbed locally and used to sustain the runaway expansion. During deflation L_r increases outwards, as thermal energy is lost locally, which causes the runaway contraction. Physical analogies are rarely fully satisfactory, yet we like one in which the stellar envelope is compared to a two-level atom. Like the atom, the envelope has two stable configurations within its central potential. One configuration is radiative (the *ground state*) and one convective (the *excited state*), and transitions between the two states occur either absorbing or emitting photons. Further flavor to the analogy is added by noting that, indeed, (part of) the absorbed photons go to ionize the heavy ions during the envelope transition off its ground level and are re-emitted when heavy ions recombine during the return to it. It is somewhat entertaining to see how so many atoms cooperate to have the whole envelope mimicking the behavior of each of them.

In summary, the envelope inflates to red giant dimensions, and deflates to dwarf size, through a runaway expansion and a runaway contraction which are both initiated when the function $W(M_r)$ becomes negative, i.e., when a thermal instability appears in the envelope, with, respectively, the surface luminosity either dropping or increasing more rapidly than the input luminosity at the base of the envelope. It is worth fully appreciating that the whole gravothermal hysteresis cycle is described under the sole driving of a varying input luminosity L_B (the trigger), while the response of the envelope is determined by the variations of thermal conductivity resulting from the recombination of the heavy ions (during inflation), and their re-ionization (during deflation). It is very important to realize that major excursions in the H-R diagram can be triggered by relatively small variations of the input luminosity. For example, the whole GTHC in Figure 2 is described under a variation of only $\sim 40\%$ in L_B. This results from the envelope being in almost neutral equilibrium when $W \simeq \pm 0$, and even small luminosity stimuli $\delta \ln L$ can produce large reactions $\delta \ln R$ when the reactivity W^{-1} is very large (Renzini 1987b). It is also worth stressing that the core size, mass, and then the gravitational potential at its boundary are all strictly constant during the GTHC, and therefore cannot have a direct role in causing the expansion to red giant dimensions, or the formation of the blue loops. Having acquired familiarity with envelope behaviors, we are now ready to consider and interpret those of the whole star.

4. AN ILLUSTRATIVE EXAMPLE: THE EVOLUTION OF A 9 $M_\odot$ STAR

The case of a 9 $M_\odot$ star with solar composition is particularly appropriate to illustrate envelope inflation and deflation episodes in a full star, since its evolutionary track presents not only the runaway expansion to red giant, but also well developed first and second blue loops. We caution, however, that all

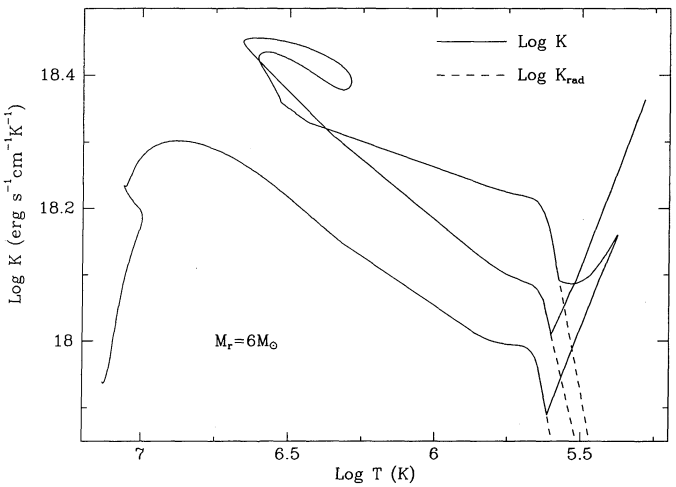

FIG. 13.—Thermal conductivity K vs. temperature at the mass coordinate $M_r = 6\ M_\odot$ for the evolutionary sequence shown in Fig. 1. The dashed line shows the radiative thermal conductivity after convection has reached the mass coordinate $M_r = 6\ M_\odot$.

these events can present quantitative and qualitative differences in stars of either different mass or composition. Some of the trends with mass and metallicity will be cursorily examined in the next section.

Figure 13 shows the whole evolutionary sequence in the $K-T$ diagram for the mass point situated at $M_r = 6\ M_\odot$. The similarity with Figure 1—although obvious—is impressive, and would remain such had we plotted K vs. T for any other mass point in the envelope. We now discuss in some detail various crucial phases of this evolutionary sequence, emphasizing similarities and differences with respect to the numerical experiment discussed in the previous section. Through this whole section by L_B we mean the luminosity in the full model at the mass coordinate $M_r = 3\ M_\odot$.

4.1. *The Pre–Main-Sequence Phase*

Our evolutionary sequence in Figure 1 starts from the zero-age main sequence (ZAMS), but it is worth beginning this section by mentioning one important aspect of the evolution prior to the ZAMS, which is described, e.g., in Iben (1965a). Stars begin their quasi-static evolution descending the Hayashi line as fully convective configurations, and during this contraction temperature and density increase throughout the whole structure. Correspondingly, in the central regions opacity and radiative gradient decrease, until a radiative core appears at the center of the star and progressively grows in mass. Shortly after the appearence of the radiative core the stellar luminosity reaches a minimum and then increases, approximately following the relation $L_S \propto R^{3\alpha-\beta} \simeq R^{-1/2}$ appropriate for freely contracting structures in radiative equilibrium (see Henyey, LeLevier, & Levée 1955). We note that this *zeroth* RGM is physically very similar to the events occurring when the contracting envelope in our numerical experiment reaches its second RGM, which marks the beginning of the blue loop. Indeed, apart from differences in time scale, observers bound to make physical measurements *inside* the envelope itself would hardly distinguish whether the star is contracting on its first approach towards the ZAMS, or descending the Hayashi line past the helium ignition in the core. We conclude that the departure from the Hayashi line during the pre–main-sequence contraction is the first manifestation of an evolutionary behavior which repeats virtually identical during the core helium burning phase, and which leads to the formation of the blue loops. *The common cause of the pre–main-sequence deflation and of blue loop formation is the growth of a radiative region below the convective envelope in which the thermal conductivity increases.* Note that during the pre–main-sequence phase $W(M_r) < 0$ from the departure from the Hayashi line, to the onset of nuclear burning in the core, when $W(M_r)$ returns to positive values as TE is reached for the first time, the final approach to the ZAMS being analogous to the F-A fraction of the GTHC.

4.2. *The Overall Contraction Phase*

During the major core hydrogen burning phase, the core contracts and the envelope expands in response to the increasing luminosity being provided by the core. However, when the central hydrogen abundance decreases below ~ 0.05, envelope expansion comes to a halt (point B in Fig. 1), the whole structure contracts, while the luminosity keeps increasing: now $W(M_r)$ is negative through the whole structure. It has been argued that during the overall contraction the evolution keeps proceeding on a nuclear time scale, as no major instability seems to arise (Weiss 1989). Weiss takes this as a counter-example for the criterion for the evolution to red giant formulated in Paper I, where the onset of the runaway expansion is attributed to the appearance in the envelope of a negative $W(M_r)$. He points out that during the overall contraction phase $W(M_r)$ is negative through the whole structure, and yet the envelope contracts. However, contrary to Weiss' claim, TE is progressively broken during the overall contraction phase, L_N drops below L_S and increasingly departs from it as hydrogen exhaustion is approached (point C). This is certainly not surprising, as fuel exhaustion inevitably implies a precipitous drop of L_N in the core, as one can see in Figure 14 which shows separately the contribution to L_N due to hydrogen burning in the convective core, and that of the burning just outside the convective core, i.e., of the igniting hydrogen-burning shell. So, one sees how nicely core burning dies out and shell burning

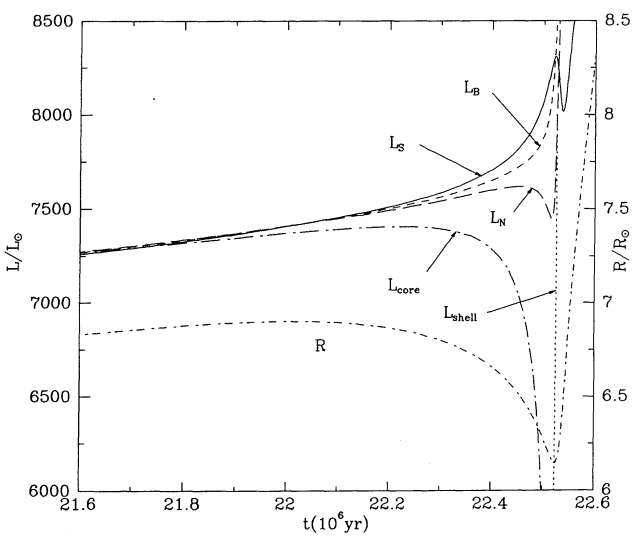

FIG. 14.—Luminosities $L_N = L_H$, L_B, and L_S as a function of time during the overall contraction phase, and through central hydrogen exhaustion and hydrogen shell ignition. The core and shell contribution to L_H are plotted separately as L_{core} and L_{shell}. Also shown is the stellar radius R.

takes over, while the rate of luminosity increase at the base of the envelope does not accelerate significantly until shell burning is well under way.

One intriguing aspect of the overall contraction is that—contrary to the previous phase—L_B and L_S keep increasing, and yet the envelope contracts. In § 2 we have noted that during the core hydrogen-burning phase the core sends two conflicting messages to the envelope: as the supporting core shrinks the envelope would tend to follow its contraction, but in the meantime the core brightening favors envelope expansion. So, during most of the core hydrogen burning phase the latter effect prevails on the former, and the envelope expands. But as hydrogen is coming to exhaustion the rate of core contraction accelerates, the envelope is progressively deprived of its mechanical support, and a time comes when this effect prevails on core brightening so that the whole envelope follows the shrinkage of the core. We have performed numerical experiments such as those described in § 3, but now keeping L_B constant and decreasing the core radius R_B. As expected, when the core shrinks so does the whole envelope.

In conclusion, the appearance of negative W's during the overall contraction phase just signal that indeed the star is progressively departing from TE, and tends to resume its secular contraction approaching again the trend $L_S \propto \sim R^{-1/2}$, that it had abandoned toward the end of the pre–main-sequence phase, when hydrogen ignited in the core. The reaction to fuel exhaustion in the core is indeed quite obvious, and the star would keep contracting indefinitely were if not for the sudden ignition of hydrogen in the shell, which bursts L_N well above L_S, thus forcing the star to reexpand. It is finally worth noting that during this stage the core shrinks much more dramatically than during subsequent evolutionary phases, and the whole star contracts. Clearly the analogy of envelope expansion to red giants with the *gravothermal catastrophe* of a star cluster really does not look physically pertinent.

4.3. *Shell-Envelope Feedback During Inflation*

Figure 15 extends beyond Figure 14 the display of the various luminosities, as the star evolves from central hydrogen exhaustion to beyond the helium ignition in the core. The ignition of shell hydrogen burning is very abrupt, and the resulting envelope expansion is so fast that initially the surface luminosity slightly drops as energy for the expansion is abstracted from the local energy flow. A similar effect can be seen in Figure 3: when L_B suddenly starts to increase the surface luminosity experiences a tiny temporary drop; the effect is also seen in Figure 14. As a general rule, L_S counterreacts to fast variations of L_B, decreasing for a short while when L_B rapidly increases, and vice versa. However, as the star readjusts in response to the hydrogen shell ignition, the W's return to positive values in the envelope, which then tends to approach TE. Strict TE is not reached though, as the rate of shell brightening forces a fairly rapid expansion of the envelope, with the accompanying abstraction of energy from the energy flow. In general, the lower the stellar mass, the closer to full TE is the star during this early hydrogen shell burning phase (see § 5.2). Soon after the ignition of the shell the envelope behaves just as in the simplified experiment described in § 3 (section A-B of the GTHC): The W's decrease in the envelope just as shown in Figure 8, until W changes sign and the runaway expansion sets in (point D in Fig. 1): the surface luminosity decreases as a result of the decreasing thermal conductivity of the envelope, and a larger fraction of the core luminosity gets trapped thus driving further expansion of the envelope.

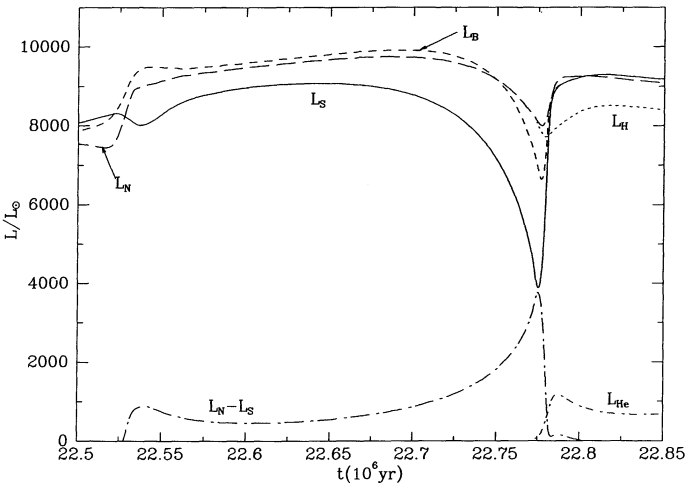

FIG. 15.—Luminosities L_N, L_B, L_S, L_H, and L_{He} from central hydrogen exhaustion to central helium ignition, and through the first red giant minimum. Also shown is the difference $L_N - L_S$ which measures the departure from thermal equilibrium. Note that $L_N = L_H$ prior to helium ignition.

All this is very similar to the case of the toy envelope experiment, yet with one important difference. In the case of the toy envelope the input luminosity L_B is maneuvered independently of what the surface luminosity is going to be. In the real stars, instead, shortly after the onset of the instability the rapid expansion of the envelope affects the strength of the hydrogen-burning shell, and both L_N and L_B decrease. A detailed inspection of the behavior of the shell shows indeed that the decreasing *weight* exerted by the envelope on the shell has the effect of reducing the rate at which shell temperature and density increase. Thus, such an increase does not compensate any longer for the decreasing hydrogen fuel abundance in the shell (i.e., for the decreasing *thickness* of the shell), and L_N starts decreasing. The causal sequence proceeds as follows: the increasing shell luminosity causes envelope expansion, thus driving it towards the thermal instability, and in turn the runaway envelope expansion causes a drop in the shell luminosity. Still, this *feedback* effect is insufficient to maintain near equality between L_S and L_N, and actually $L_N - L_S$ increases until TE equilibrium is restored when the envelope becomes convective (see Fig. 15). *The weakness of the shell-envelope feedback is a manifestation of the partial decoupling of the already compact core from the expanding envelope*, a decoupling that can only become more pronounced as the envelope expands. *Were it not for the onset of convection, the envelope would expand forever.*

The burning shell being located just interior to the boundary between the contracting core and the expanding envelope, its strength L_N is influenced by the relative rate of core contraction and envelope expansion, and any change in either such rates can immediately produce a variation of L_N. Although temperature and density in the shell keep increasing, during the runaway the latter effect dominates and L_N decreases. But core contraction regains the lead when upon arrival on the Hayashi track the expansion slows down, TE is restored, and thus L_N resumes increasing. The return of the envelope to TE proceeds just as in the case of the toy envelope experiment,

with the behavior of the function $W(M_r)$ around the first RGM (point E in Fig. 1) being just as that shown in Figure 11.

There are two other features worth noting in Figure 15. (1) The decrease of L_S substantially anticipates the decrease of L_N and L_B, which further signals that the instability starts indeed in the envelope itself, and the shell drop *follows*. (2) Seemingly, at arrival on the Hayashi line L_S starts increasing *before* L_N and L_B do so, which again signals that it is indeed the rate of envelope expansion which drives the luminosity evolution of the shell.[6]

4.4. *Shell-Envelope Feedback During Deflation*

Following full helium ignition (point F in Fig. 1), the inner part of the hydrogen-exhausted core initiates a very slow expansion which will last through most of the helium-burning phase. This is a result of the burning core working as a *breeder* reactor during this stage: as triple-α reactions produce ^{12}C, the subsequent channel $^{12}C(\alpha, \gamma)^{16}O$ releases an increasing amount of energy, and the inner core is forced to expand. The temperature in the hydrogen-burning shell correspondingly decreases, so does the luminosity L_H released by the hydrogen shell, and the star descends along the Hayashi track. The situation is now very similar to that experienced by the toy envelope during the power-down section of the GTHC. Shortly after the base of the envelope has returned to radiative equilibrium, negative W's appear just as shown in Figure 12 (point G in Fig. 1), TE is broken, and the envelope starts losing much more energy than it receives from the core: the runaway deflation has started. As we have pointed out for the feedback effect during inflation, also now there is an important difference with respect to the case of the toy envelope. In fact, envelope contraction affects the strength of the shell L_H (and therefore L_B), which—though with a short delay—follows the increase in L_S. All these trends are very clearly illustrated in Figure 16. However, contrary to the case of the runaway inflation in which shell and envelope become more and more decoupled with expansion, as one may expect during deflation shell and envelope become more and more coupled to each other, until L_N closely tunes itself to L_S and TE is restored (point H in Fig. 1). This is a fairly abrupt event, as testified by the sharp bend of the track at point H, when contraction effectively ceases for a while. It is easy to realize how such fine tuning is accomplished by the star: insofar L_N is substantially smaller than L_S there is fast contraction, and therefore fast increase of L_N toward L_S. However, feedback alone cannot allow L_N to increase above L_S, otherwise the envelope would expand, and in turn there would be no increase of L_N. As a result of this self-tuning mechanism L_N approaches very closely L_S, still remaining slightly below it by the right amount needed for the slow contraction of the envelope to balance the slow expansion of the inner core, in such a way that L_N increases just in pace with L_S. The core helium-burning stage on the blue side of the H-R diagram provides a very nice example of a self-regulated, complex physical system.

Before discussing the termination of the blue loops, we like to show in Figure 17 the run of L_r inside the star for several models during both inflation and deflation. As one can see, up to 50% of the nuclear luminosity can be absorbed to expand the envelope during inflation (phase DE), while during deflation (phase GH) up to 15% of the surface luminosity comes from the rapid contraction of the envelope.

4.5. *Shell-Core Coupling and the Termination of Blue Loops*

In § 4.4 we have seen how the shell strength is coupled to the behavior of the core, which slowly expands during most of the

[6] Both these features are evident in Fig. 6 of Iben (1965b), and it was indeed by meditating this figure that we first realized that a runaway radiative energy trapping in the envelope was the cause of the transition to red giant.

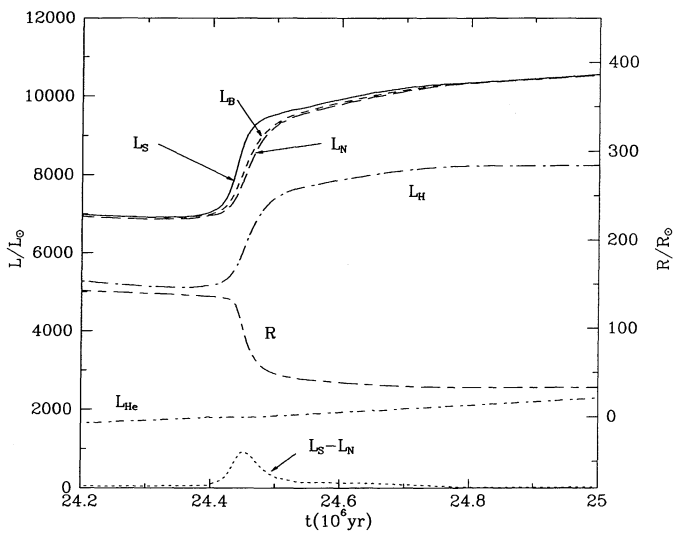

FIG. 16.—Luminosities L_N, L_H, L_{He}, L_B, L_S, and the stellar radius R from the second red giant minimum, through the runaway deflation, to the restoration of thermal equilibrium. Also shown is the difference $L_S - L_N$ which measures the departure from thermal equilibrium.

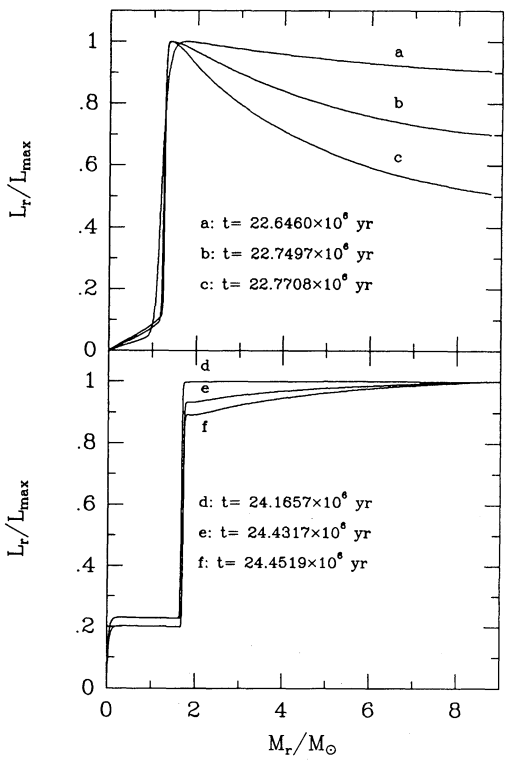

FIG. 17.—Luminosity L_r vs. M_r for representative models during inflation (*upper panel*) and during deflation (*lower panel*). The evolutionary epoch of each configuration is indicated. Note that the energy produced in the hydrogen-exhausted core comes from gravitational contraction during inflation (*upper panel*), and from helium burning during deflation (*lower panel*).

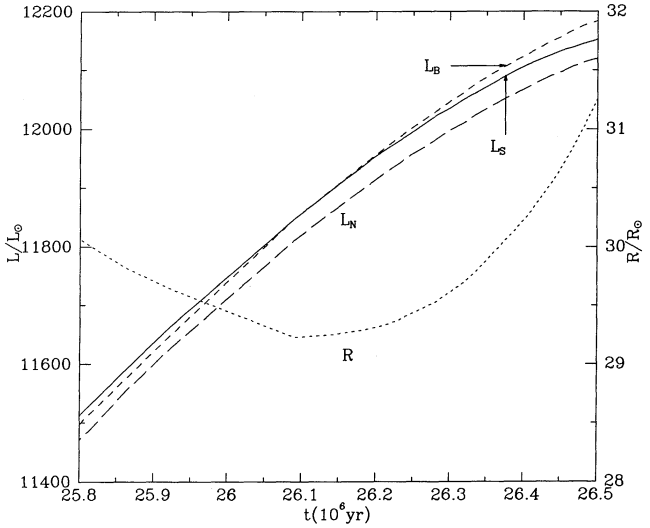

FIG. 18.—Luminosities L_N, L_B, and L_S, and the stellar radius R through the termination of first blue loop.

core helium-burning phase. This slow expansion progressively decelerates until it ultimately turns to contraction as the $^{12}C(\alpha, \gamma)^{16}O$ reaction reaches equilibrium, the ^{12}C abundance in the core starts declining, and eventually the contraction accelerates as helium exhaustion in the core is approached. Thanks to the strong coupling between core and shell, core contraction results in a faster and faster increase of the shell luminosity L_H and therefore of L_N as a whole. As shown in Figure 18, eventually the nuclear luminosity[7] exceeds the surface losses, envelope contraction correspondingly ceases, and the stellar radius starts to increase. Past point I in Figure 1, for a while the situation in the envelope is quite similar to that encountered during the early shell hydrogen-burning phase (between point C′ and point D in Fig. 1), with positive, both radially and secularly decreasing W's through the whole envelope. Seemingly, under the stimulus of the increasing nuclear luminosity soon a time comes when $W(M_r)$ vanishes near the surface and then becomes negative, and a second runaway expansion toward red giant dimension sets in. The behavior of the envelope during this expansion would be very, very similar to that previously followed during the first thermal instability, were if not for a sequence of dramatic events taking place in the core and propagating through the envelope, which are described in the next section.

4.6. *The Second Blue Loop*

Figure 19 displays the behavior of the various luminosities through helium exhaustion in the core, helium ignition in the shell, the second blue loop, and the expansion to the AGB (i.e., from slightly past point K to beyond point L). Helium-shell ignition is quite violent, and matter starts expanding rapidly, away from the igniting region (see Iben 1965b). As the expansion front breaks through the hydrogen-burning shell, temperature and density in the shell drop, and so does the rate of energy release L_H: quickly the hydrogen shell is effectively extinguished. All these events take place while the star has already initiated its second runaway inflation, as indicated by the sizable departure of L_S from L_B in Figure 19. Helium exhaustion in the core and ignition in the shell cause by themselves a violent departure from TE, but now this happens while the envelope is already far from TE, and the resulting evolutionary behavior of the star is quite complicated indeed: certainly not one which could be understood solely with the aid of TE models (for a detailed description of the events associated to the second blue loop see Becker 1981). Yet, we believe that the behavior of the star and its loop in the H-R diagram can be understood by just considering the variation of the input luminosity at the base of the envelope L_B, and the corresponding reactions of the envelope. The variations of the core size have no appreciable (mechanical) influence on the envelope, its volume at this stage being virtually negligible compared to that of the envelope.

As a result of core extinguishment, helium-shell ignition, and hydrogen-shell extinguishment, the nuclear luminosity $L_N = L_{He} + L_H$ first decreases, then presents a shortlived peak associated to the power-up of the helium shell and the power-down of the hydrogen shell, and finally increases again following the secular increase of the strength of the helium shell L_{He}, which ultimately remains the only active energy source in the star (see Fig. 19). However, already at $M_r = 3\ M_\odot$ the short peak in L_N is washed out by energy absorption mainly in the expanding helium shell itself, and the input luminosity L_B presents only one minimum. As already mentioned in § 4.3, in general the surface luminosity counterreacts to fast variations of L_B: when L_B drops rapidly the envelope loses more energy than it gets from the core, and is forced to contract and to brighten, such as in the case of the overall contraction phase. The same effect gives rise to the turnaround at point J, when the rate of decrease of L_B strongly accelerates, and so the second blue loop is initiated. However, soon L_B resumes increasing again, and again the envelope conterreacts: as it turns to expansion, energy is abstracted from the flow and L_S starts decreasing (point K). It is important to realize that the redistributions of the energy production among the various burning regions are all intimately connected to each other, i.e., it is the core extinguishment which causes the helium-shell ignition, which in turn switches off the hydrogen shell. So, quite naturally this series of events produces a minimum in L_B

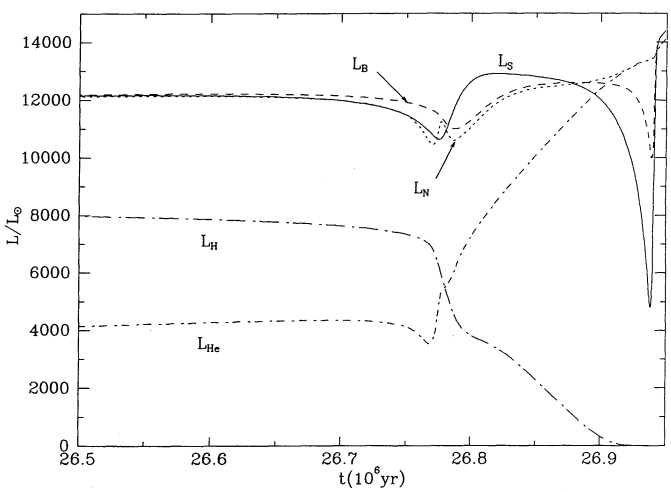

FIG. 19.—Luminosities L_N, L_H, L_{He}, L_B, and L_S through the second blue loop.

[7] Actually, a non-negligible gravitational contribution from the contracting core helps the core luminosity to exceed the surface luminosity.

shortly after the star has initiated its runaway inflation toward the AGB: in the midst of this runaway the envelope is then caught by a stimulus to deflate (the drop in L_B) and shortly thereafter by another stimulus to inflate (the subsequent increases of L_B), and it is in response to this complex series of stimuli that the envelope describes its second blue loop. Finally, as the shell luminosity keeps increasing the star initiates and concludes on the AGB its third runaway inflation, from point K to L, which corresponds to the third RGM. Helium exhaustion in the core, helium-shell ignition, hydrogen-shell quenching, and envelope inflation and deflation are all intimately accompanied by strong local and global deviations from TE. This explains why little insight, if any, can be gained on second blue loops from models constrained to be in TE.

After several attempts, by properly maneuvering L_B we have succeeded in producing a variant of the GTHC discussed in § 3, in which the toy envelope describes full first and second blue loops. From these experiments we learned that the morphology of the second blue loop is extremely sensitive to the precise run with time of the input luminosity L_B, and in particular on the phasing of its minimum with respect to the second runaway inflation. We believe that the systematics of second blue loops (which escaped so far a physical understanding, see Backer 1981) can be fully understood using the conceptual tools that we have developed here, but a more detailed discussion of this evolutionary phase goes beyond the scope of this paper. Suffice to mention that great variance of the morphology of the second blue loop is obviously expected, given the extremely delicate interplay between core, shell, and envelope events, each characterized by slightly different time scales. To avoid ambiguous terminologies, we shall refer to the "second blue loop" for the events caused by the helium-shell ignition, even in those cases in which the star does not experience a well developed "first blue loop" during the core helium-burning phase. An interesting application of these concepts will be presented in § 5.4.

4.7. *The Criterion for Thermal Stability*

During the strong-feedback fraction of the core helium-burning phase (i.e., between point H and point I in Fig. 1) the surface luminosity increases, the radius decreases, and then $W(M_r)$ is negative in the envelope. Yet the star is extremely close to its TE, and correspondingly the evolution proceeds on a nuclear time scale. We have seen that the condition $W > 0$ was necessary and sufficient to ensure thermal stability in the case of the toy envelope. More generally, this is so when the shell-envelope feedback is absent or weak. During core helium burning, instead, the condition $W > 0$ is violated but the envelope can be very close to its TE. Clearly, a more general stability criterion is required when the feedback effect is important. It is easy to realize that thermal equilibrium will be ensured even when $W < 0$, provided that by contraction or expansion the energy generation $L_N(M_r)$, respectively, increases or decreases more rapidly than energy losses L_r, i.e.,

$$\frac{\delta \ln L_r}{\delta \ln r} - \frac{\delta \ln L_N(M_r)}{\delta \ln r} > 0 \qquad (13)$$

or

$$W(M_r) - W_N(M_r) > 0\,, \qquad (13')$$

where $L_N(M_r)$ is the nuclear luminosity produced inside the sphere of mass M_r, and we have introduced the *nuclear W-function* $W_N(M_r)$. Although in principle equation (13) could ensure thermal stability in the case of an expanding configuration with decreasing surface luminosity (provided L_N decreases more steeply than L_r), in practice we are not aware of any concrete case in which such a situation is actually realized in the course of stellar evolution. Therefore, inequality (10) is both a necessary and a sufficient condition for the thermal stability of evolutionarily *expanding* envelopes, as inequality (11) is for their thermal instability. Moreover, in all cases of week shell-envelope feedback $W_N(M_r)$ is small in the envelope, and again (13) becomes equivalent to (10).

We finally note that the validity of condition (13) is not limited to stellar envelopes, but holds true for every point in the star. In particular, it applies the thermal stability of burning cores, such as in the case of hydrogen-burning cores which contract and yet become more luminous. Their thermal equilibrium is maintained thanks to the large negative value of $W_N(M_r)$ in the core, i.e., by the *strong feedback* of core contraction on the nuclear reaction rates. The criterion applies also to the case of a thermonuclear flash, such as the core helium flash or the helium-shell flashes on the AGB. Indeed, in a flashing region $W_N(M_r)$ is positive and extremely large, i.e., $W_N(M_r) \gg W(M_r)$, condition (13) is violated, and the star is indeed experiencing a most dramatic departure from TE, while still maintaining its hydrostatic equilibrium. As stated explicitly, Paper I dealt only with envelopes, and the stability criterion (10) was not designed to apply also to stellar cores. This caused some misunderstanding (e.g., Weiss 1989), which should now be completely ovecome, as the general stability criterion applies to envelopes as well as to cores.

4.8. *Summary of Main-Sequence to AGB Evolution*

In this final subsection we present two evolutionary diagrams which provide a comprehensive description of the evolution of the star in a way which very explicitly allows to identify the main burning stages in TE, as well as the crucial evolutionary phases in which TE is broken and the star can undergo extended excursions in the HR diagram. Figure 20, analogous to Figure 5 for the GTHC of the toy envelope, displays the evolution in the $L_S - L_B$ plane, with $L_B = L_r(M_r = 3\ M_\odot)$. Of course, TE is ensured when the star evolves close along the line $L_S = L_B$, while departures from such line correspond to major thermal instability phases. When reading Figure 20 a real time conparison with Figure 1 will help to fully understand the development of the varius evolutionary events. For this reason, the lettering along the sequences displayed in the two figures refers exactly to the same evolutionary epochs.

Evolution from A to B corresponds to core hydrogen burning near the main sequence, and TE is very closely fulfilled. The star begins departing from TE at point B, i.e., at the onset of the overall contraction phase. At point C hydrogen shell burning ignites, and the rapid increase in L_B so produced forces the envelope to expand, energy is abstracted from the flow, and L_S drops. At point C′ the star begins to recover from the rapid readjustment caused by shell ignition, and start reapproaching TE (phase C′ to D). Strict TE is not reached, though, but it is so in less massive stars during this phase (see § 5.2). The opacity-related thermal instability arises in the envelope at point D, and the star inflates to red giant dimensions until the Hayashi line is reached at point E. Then TE is rapidly restored throughout the whole star, until helium is ignited at point F. The phase F-G corresponds to quiet, TE helium burning in the

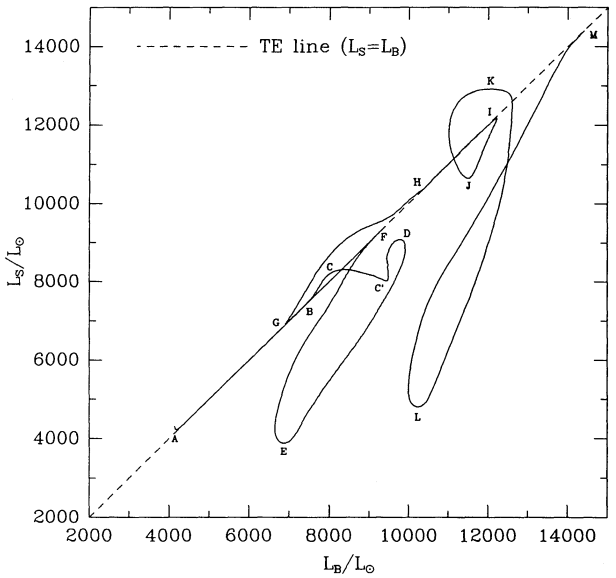

FIG. 20.—Whole evolution of the 9 $M_\odot$ star in the $L_B - L_S$ plane. The letters identify the same evolutionary events as in Fig. 1. The straight dashed line at 45° is the locus of models in thermal equilibrium (i.e., $L_S = L_B$).

core as a red giant close to the Hayashi line. As deconvectivization at the base of the envelope proceeds, the deflation thermal instability suddenly breaks out at point G and proceeds to point H, when TE is restored thanks to the shell-envelope feedback. From H to I the star evolves through its major, TE helium-burning phase as a blue giant. Near point I helium approaches exhaustion in the core, and shortly thereafter the envelope becomes thermally unstable on its own for the second time, as it did before at point D. From I to J the runaway inflation proceeds, until the fall and rise of L_B causes the second blue loop JK. At K the envelope is directly driven to its own inflation thermal instability for the third time, and the final expansion to the AGB can resume, reaching the Hayashi line at point L, and restoring its full TE at point M. Note that in the segments DE, IJ, and KL, i.e., during the envelope runaway expansion, not only L_S (as in Fig. 3), but also L_B decreases. In the first two cases this is mainly a result of the shell-envelope feedback, as the strength of the hydrogen shell decreases because of envelope expansion. In the third case the hydrogen shell is actually extinguished, and the decrease of L_B results from local expansion. During the second blue loop the evolutionary line in the $L_S - L_B$ plane crosses two times the TE line $L_B = L_S$, shortly after point J and after point K. Formally, the corresponding configurations are in TE, but are not so those immediately preceding or those immediately following them, and therefore one cannot say that TE has actually been restored in the envelope.

In Figure 21 the time evolution of the surface value of $W - W_N = W(M) - W_N(M)$ is displayed, together with the evolution of the stellar radius R. Again, the lettering identifies the main evolutionary events as in Figure 1 and Figure 20. Here we see at work the thermal stability criterion introduced in § 4.5, and one can directly appreciate that negative values of $W - W_N$ are indeed associated with rapid expansions or contractions of the star, which, respectively, take place when either more energy is produced in the core than can be transferred outwards by the envelope, or vice versa the envelope radiates more energy than can be produced by the core. Note that at local maxima and minima for stellar radius $\delta \ln R = 0$, and the function $W - W_N$ presents poles (unless the luminosity time derivatives vanish as well). This happens at the points B, C, I, J, and K, which all coincide or closely correspond to main departures from TE. It is fully apparent from Figure 21 that the star is in TE through most of its life, and departs from TE only a few, yet crucial times during its whole evolutionary history. These stages coincide with major readjustments of the stellar structure, which take place on a thermal time scale. In summary, when the star is very close to TE then $W - W_N$ is small and positive, when it is negative the star progressively departs from TE, and when it is positive and large the star can still be far from TE but is rapidly approaching it.

In summary, we can distinguish five basic evolutionary behaviors, whose main characteristics can repeat in the course of evolution. Three such behaviors correspond to configurations in thermal equilibrium: (1) Both L_S and R increase ($W > 0$) and the envelope is radiative, such as during the phases AB, C'D, and shortly after point I. (2) Both L_S and R increase, or decrease ($W > 0$) and the envelope is convective, such as during the Hayashi phases EF, FG, and LM. (3) L_S increases and R decreases, $W < 0$ but $W - W_N > 0$, which happens when there is a strong shell-envelope feedback (phase HI). The two last behaviors correspond to major departures from TE, and are characterized by negative values of both W and $W - W(M_r)$: (4) runaway inflations with decreasing L_S while R increases, such as during phases DE, IJ, and KL; and finally (5) runaway deflations with increasing L_S and decreasing R, such as during the pre–main-sequence phase and phases BC, GH, and JK.

5. UNDERSTANDING SUBTLE EFFECTS

Over the years, several correlations between evolutionary behaviors and stellar parameters have been phenomenologically noticed, given the large number of evolutionary sequences accumulating in the literature, and still many of such relations

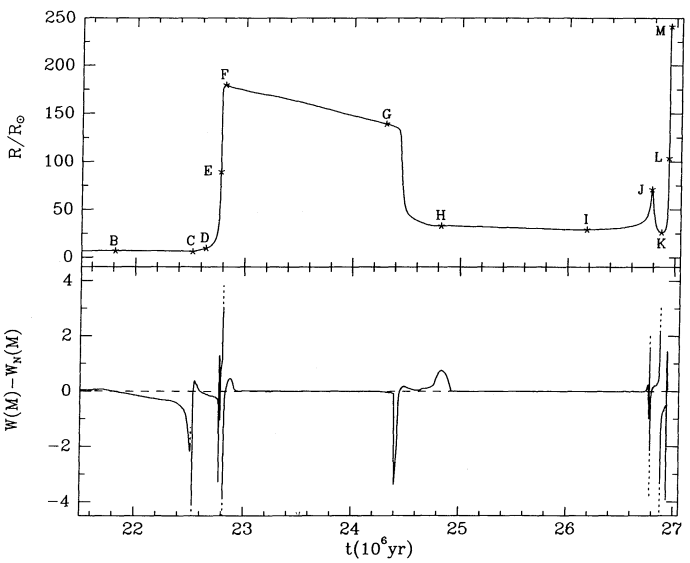

FIG. 21.—Time evolution of the stellar radius and of the thermal stability diagnostic function $W - W_N$, from slightly before the beginning of the overall contraction phase, all the way to the AGB. The letters identify the same evolutionary events as in Fig. 1. Note that poles are present at minima and maxima of the stellar radius.

have not been physically explained. Prototypical in this regard is the case of blue loops. In this section we discuss blue loops and other similar cases, in light of the understanding of stellar behaviors so far achieved in this paper.

5.1. "*To Loop or not to Loop*"

With this title Kippenhahn & Weigert (1990, chap. 31.4) seem to express their embarrassment for blue loop formation still escaping their comprehensive understanding. "The red giant structure [being] a configuration adopted by hot matter placed in an external gravitational field" (Fujimoto & Iben 1991) the attention of Kippenhahn & Weigert—and many others before them—may have been attracted more by the need of ensuring hydrostatic equilibrium in a gravitational field, than by the need to transfer through the star and radiate away the energy produced in the stellar core. This may explain why their attention focused on the gravitational potential at the core boundary Φ_c, rather than on the luminosity radiated by the core, L_B. In § 3 we have demonstrated that loops are produced under the sole action of a variation of L_B, while Φ_c is kept strictly constant. So for saying, *the envelope barely knows what Φ_c is, but knows very well how much luminosity (L_B) it is asked to get rid of.* Still, one has to bear in mind that in the approach of Kippenhahn & Weigert the core mass and size (and then Φ_c) affect the strength of both core and shell nuclear sources, and therefore of L_B. After all there is a link between envelope behaviors and Φ_c, but this link is indirect and is mediated by the luminosity.

In this section we try to account for many heretofore unexplained properties of blue loops by primarily considering how various factors can affect the core luminosity L_B, and from the evolution of L_B deduce the expected behavior of the envelope. We also keep in mind that blue loops are usually initiated by the runaway deflation of the envelope: i.e., deviations from TE are intimately connected to the blue loop phenomenon, which therefore can barely be understood by restricting themselves to the consideration of pure TE models (as done by Kippenhahn & Weigert 1990, and Lauteborn, Refsdal, & Weigert 1971). Such models say which are the possible TE configurations of the star, for example indicating that both red giant and blue giant configurations are possible during the core helium-burning phase. But can hardly say when, how, and why a star will at some point make a fast transition from one configuration to the other.

During the core helium-burning phase, the stellar nuclear luminosity first decreases, reaches a minimum, and then increases. As described in § 4, this is mainly a result of a modest core expansion reducing the strength of the hydrogen shell, and later of core contraction as helium exhaustion in the core is approached, with the hydrogen shell strenghening again. Superposed on this trend, the shell-envelope feedback effect can significantly anticipate the time when the minimum nuclear luminosity $L_N^{\min}$ is reached. From the experiments with toy envelopes we have learned that if the luminosity at the base of the envelope is reduced below a critical value $L_{\rm loop}$, then a blue loop is initiated. Since in a whole star (complete of core and envelope) $L_B \simeq L_N$, it follows that an extended blue loop is formed if $L_N^{\min} < L_{\rm loop}$, i.e., if the nuclear luminosity decreases below the *threshold* $L_{\rm loop}$.[8] Conversely, if $L_N^{\min} > L_{\rm loop}$, then there will be little departure from the Hayashi line, so that the star will first slowly descend down to $L_S \simeq L_N^{\min}$, and then climb back again along the Hayashi line. It follows that anything affecting either $L_N^{\min}$ or $L_{\rm loop}$ can potentially affect also the formation and extension of the blue loops. Since both $L_N^{\min}$ and $L_{\rm loop}$ are functions of mass, composition, and input physics, we see that quite a variety of situations may arise, as phenomenologically well-known. With this key in our hands, we now list and briefly discuss the role of several factors known to affect the blue loops. This will be little more than a cursorily qualitative anticipation, while we intend to postpone to further papers a more detailed exploration of the various effects.

5.1.1. *Blue Loops and Convective Overshooting*

When large overshooting is assumed at the edge of convective cores during the main-sequence phase, blue loops are dramatically reduced or suppressed. Instead, the loops can magically reappear if sizable overshooting at the base of convective envelopes is also assumed (Matraka, Wassermann, & Weigert 1982; Chiosi 1990; Alongi et al. 1991; Stothers & Chin 1991). None of these effects has been physically explained so far. The blue loop-overshooting connection can easily be understood when considering the effect of overshooting on the luminosity evolution during the core helium-burning phase. As is well-known, models with overshooting are characterized by larger hydrogen-exhausted cores (i.e., by larger M_B/M ratios) and are correspondingly brighter than models without overshooting.This applies to both $L_{\rm He}$ and $L_{\rm H}$. Therefore, also $L_N^{\min}$ will be larger, while no appreciable effect of core overshooting is predicted on $L_{\rm loop}$, which is basically a property of the envelope. It follows that the increase of $L_N^{\min}$ can bring it above $L_{\rm loop}$, and thus suppress the blue loop.

The action of overshooting below the base of the convective envelope is somewhat more intricate. As the star first arrives on the RGB, the envelope convection penetrates inwards giving rise to the so-called *first dredge-up*, thus generating a modest discontinuity in the hydrogen abundance. Later, the discontinuity is left behind as envelope convection recedes. When the hydrogen-burning shell approaches the discontinuity (but *before* actually reaching it), models experience a modest luminosity drop, while soon the star's luminosity resumes to increase as the shell actually burns through the discontinuity (see Sweigart, Greggio, & Renzini 1990 for a physical explanation of the phenomenon). It is easy to realize that when overshooting is allowed below the base of the convective envelope the chemical discontinuity becomes larger and is residuated deeper in the star. Correspondingly, the hydrogen shell reaches the discontinuity at an earlier evolutionary stage, and the size of the luminosity drop is larger. As shown by Sweigart et al. (1990), in stars less massive than ~ 2 $M_\odot$ the hydrogen discontinuity is reached before helium ignition in the core, and envelope overshooting will have no appreciable effect on the formation of loops. Conversely, in more massive stars the shell can reach the hydrogen discontinuity during helium burning in the core, while the star is descending along the Hayashi track, and thus the luminosity decrease is larger than it would have been in absence of overshooting, i.e., $L_N^{\min}$ can be reduced. If the new $L_N^{\min}$ is below $L_{\rm loop}$ a blue loop can be formed.

More generally, for the same physical reason the loop formation and extension can be affected by any other process able to alter the chemical stratification in the region through which the hydrogen shell burns through past helium ignition. In particular, this is the case for convective (and/or semiconvective)

[8] The actual value of $L_{\rm loop}$ may depend slightly on the rate with which L_N is decreasing.

shells which may appear above the hydrogen-burning shell prior to the helium ignition, and whose location and size depend on whether the Schwarzschild or the Ledoux criterion is adopted (e.g., Lauteborn et al. 1971). In general, the larger and deeper the hydrogen discontinuity, the larger the luminosity drop as the hydrogen-burning shell approaches the discontinuity, and hence the larger the chance for the formation of an extended blue loop.

5.1.2. *Blue Loops and Mass Loss*

It is well-known that pulsation theory tends to give Cepheid masses which are somewhat smaller than predicted by standard evolutionary models. Sometimes, in the attempt of reconciling the two theories, mass loss prior to the Cepheid phase has been invoked, but with the disappointing result that even a modest amount of mass loss may be sufficient to suppress the Cepheid loops. The effect can be easily understood when considering that the action of mass loss is somehow similar to that of core overshooting. Indeed, a given core mass to total mass ratio M_B/M—and the loop extension implied by it—can either be produced by increasing M_B for given total mass M (overshooting), or by decreasing M for fixed M_B (mass loss). Therefore, both core overshooting and mass loss tend to suppress the blue loops as both increase the M_B/M ratio and along with it the $L_N/L_{\rm loop}$ ratio, thus favoring the case $L_N^{\rm min} > L_{\rm loop}$. Of course, mass loss (or overshooting) may resuscitate the loop, as the star has ultimately to turn blue if most of the hydrogen-rich envelope is either stripped away, or mixed to the core and burned out.

5.1.3. *Blue Loops and the* $^{12}C(\alpha, \gamma)^{16}O$ *Reaction*

It has been known for a long time that increasing the cross section of the $^{12}C(\alpha, \gamma)^{16}O$ reacton has the effect of lengthening the extension of blue loops (Iben 1967; Brunish & Becker 1990). This effect can readily be understood when considering that the higher efficiency of this reaction is equivalent to a larger disposal of nuclear energy, as more energy per gram of helium can be extracted. The core helium-burning phase is correspondingly prolonged, the helium exhaustion in the core is delayed, and so is the moment when $L_B \simeq L_N + L_g$ exceeds L_S, contraction stops and the star reexpands (point I), i.e., a larger $^{12}C(\alpha, \gamma)^{16}O$ cross section allows the star to evolve further to the blue, thus increasing the extension of the blue loop. As one can see from Figure 18 the gravitational luminosity of the core (L_g) gives a non-negligible contribution to L_B.

5.1.4. *Blue Loops and Semiconvection*

Quite similar is the effect of semiconvection and/or convective overshooting at the edge of the helium-burning convective core. By bringing fresh helium fuel into the core, both processes prolong the core helium-burning stage and delay the time when $L_B \simeq L_N + L_g$ first exceeds L_S, and the star reverses the direction of its evolution in the H-R diagram. The FUJIMO code that we have used to construct the sequence shown in Figure 1 has been modified to allow for some advancement of the convective boundary during the core helium-burning stage (such as in Castellani, Giannone, & Renzini 1971), but implementing a full semiconvection routine was beyond the scope of the present investigation. Performing various numerical experiments we have noticed that the time and location of the turnover at point I is extremely sensitive to the rate at which helium is mixed into the core. When the central helium abundance has decreased below $\sim$0.15, as the ingestion rate is decreased below a critical value the blue loop is immediately terminated. Since models spend close to point I a large fraction of the core helium-burning stage away from the Hayashi line, it follows that the time spent by the models within the Cepheid instability strip can be dramatically sensitive to minor variations in the rate of helium ingestion in the core. This circumstance seriously limits the predicting power of the models insofar the theoretical period distribution of the Cepheids in a given stellar population is concerned. We conclude that, besides the successful prediction of the gross features of the period distributions (such as their dependence on metallicity, see Becker, Iben, & Tuggle 1977), there would be little astrophysical sense in trying to reproduce finer details of such distributions.

5.2. *The Dependence on Mass*

So far we have described and commented the evolution of a 9 $M_\odot$ star, while in this section we cursorily discuss the mass dependence of the track morphology, with particular attention on the different development of envelope thermal instabilities in stars of different masses. Much of the systematics with mass of evolutionary track morphology follows from the fact that the main sequence crosses the H-R diagram diagonally, while the Hayashi line is nearly vertical. Correspondingly, the more massive stars have to cross the whole diagram before reaching the Hayashi line, while less massive stars need to cover a much shorter distance to reach the base of the RGB. Seemingly, the locus occupied by *blue* core helium-burning stars runs nearly parallel to the main sequence (see Iben 1967), and therefore the extension of the blue loops is much wider in massive stars than it is in low-mass stars. Schematically, massive stars have more *room* at their disposal in the H-R diagram than low-mass stars do (see, e.g., Fig. 15 in Maeder & Meynet 1989). A second key helps in understanding the gross features of the track morphology: the ratio of the nuclear to the thermal time scale decreases with increasing mass as $\sim 1/M$, and envelope reactions tend to lag behind core events. This makes the connection between the structure of the core and the position of the star in the H-R diagram more loose in massive stars than it is in intermediate- and low-mass stars.

The systematics with mass of the overall contraction phase is well-known. It simply disappears in low-mass stars, along with convective cores, as the near contemporary exhaustion of hydrogen in a zone of finite size (indeed, the convective core) is needed to produce it. Below $\sim$1.1–1.2 $M_\odot$ core hydrogen-burning stars do not have convective cores, hydrogen exhaustion in the core is more diluted in time, and no overall contraction phase takes place.

We now turn to the phase C′-D, which immediately precedes the star of the runaway inflation. We already noted in § 4.3 that the 9 $M_\odot$ model approaches TE without really reaching it during this phase. In less massive stars the hydrogen shell ignition is more gentle, and—even more important—there can be a prolonged thick hydrogen shell-burning phase, prior to the nearly isothermal core reaching the Schönberg-Chandrasekhar limit (see Iben 1965b, and references therein). Correspondingly, the lower the mass, the longer the C′-D phase, and the closer the approach of the star to TE. This is illustrated in Figure 22, showing indeed that in 2 and 3 $M_\odot$ stars almost strict TE is established during this phase, until TE is broken by the radiative-flow trapping in the envelope, and the extended loop in the $L_S - L_N$ diagram is initiated. Conversely, at the opposite extreme, in stars more massive than 9 $M_\odot$ the approach to TE

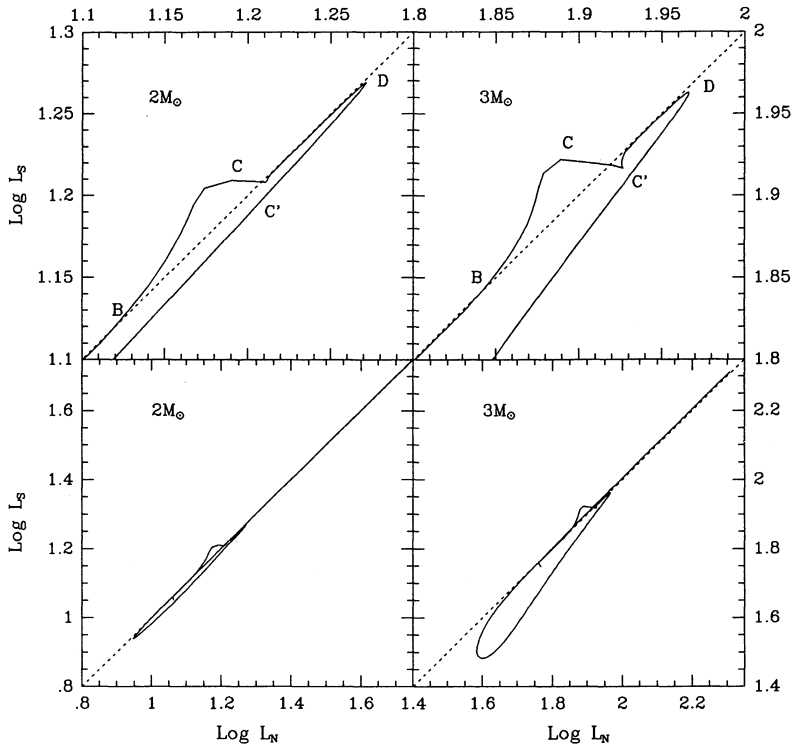

FIG. 22.—L_S vs. L_N for 2 and 3 $M_\odot$ evolutionary sequences from Sweigart et al. (1989). The upper panels display a blow-up of the section including the overall contraction phase (BC), the hydrogen-burning phase in a thick shell (C'-D), and the beginning of the runaway expansion (after point D). The straight dashed line at 45° is the locus of models in thermal equilibrium (i.e., $L_S = L_B$). Note in the lower panels the evolution in thermal equilibrium along the red giant branch, which begins at the absolute minimum of both L_S and L_N.

after shell hydrogen ignition is less and less successful, the C'-D section of the loop becomes shorter and shorter (as one can figure out by extrapolating the trend from Figs. 22 and 20), until it vanishes completely. For even more massive stars hydrogen shell ignition is so violent that the stellar envelope is pushed directly into its thermal runaway expansion without even approaching TE. Therefore, in such stars the runaway inflation initiates while the envelope is already far from TE (because of the quick hydrogen shell ignition). This makes the behavior of massive stars more difficult to interpret, as two independent cases of departure from TE overlap one another: hydrogen ignition in the shell, and radiative-flow trapping in the envelope.

Systematic differences with mass exist also for the subsequent runaway inflation phase D-E. In general, the violence of the runaway decreases with decreasing mass, i.e., the relative energy absorption in the envelope $(L_B - L_S)/L_B$ decreases. It does so to the extent that for masses below $\sim 1\ M_\odot$ (the actual value depends on metallicity) the drop in surface luminosity typical of the D-E phase vanishes, and so does the runaway expansion itself. Low-mass stars become red giants without ever departing from TE, and gently approach the RGB and climb along it until helium ignites in the core. This follows from that fact the low-mass stars begin their evolution already close to the Hayashi line, and their envelope becomes convective *before* the thermal instability has a chance to take place: the early establishment of convection suppresses the thermal instability of the envelope. This behavior can be understood noting that for decreasing stellar mass the difference in radius between the ZAMS configuration and the RGB configuration at the base of the Hayashi track decreases, and therefore so does the energy difference between the radiative and the convective configurations of the envelope. Thus, less energy needs to be absorbed in the radiative to convective transition, to the extent that TE can be maintained through the transition itself. Yet, we anticipate that a runaway expansion with the associated drops of L_S can be produced also in low-mass stellar models, provided that the energy difference between the two configurations is artificially increased. This can be accomplished by appropriately reducing the efficiency of convection. It suffices for this experiment to reduce the mixing length parameter substantially, e.g., from the canonical value $\lambda/H_P \gtrsim 1$ required to fit observed stellar radii, down to say ~ 0.1.

We finally comment on the mass-dependence of the first blue loops. As already noticed, the lower the mass, the narrower is the effective temperature (radius) range allowed to core helium-burning models, and therefore the less dramatic is the envelope deflation during phase G-H. This implies in less massive stars a less dramatic departure from TE during phase G-H. Eventually, such a departure becomes so small as to pass completely unnoticed, and almost strict TE holds through the whole core helium-burning phase: the red and blue sections of this phase have merged. Again, it may be more difficult to understand the formation of blue loops by restricting the study to lower mass stars which do not develop a macroscopic runaway deflation episode. This may not be the whole story, as the systematics with stellar mass of $L_N^{\min}$ versus $L_{\rm loop}$ remains to be investigated.

5.3. *The Dependence on Metallicity*

We have so far restricted our discussion to stars of near solar composition. However, the recognition that stellar envelope runaway expansions and contractions are primarily driven by

a metal opacity-driven instability, allows a deeper physical understanding of a phenomenologically well-known systematics of track morphology with metallicity. We emphasize that in no other proposed explanation of *why stars become red giants* one has ever attempted to answer the question "*why very metal poor stars do NOT become red giants?*," a question which instead finds a most natural answer in the frame of our physical interpretation.

Basically, when decreasing the metal abundance the metal contribution to opacity decreases, both α and β decrease, and so does the violence of runaway inflations. Figure 23 very clearly illustrates the case: the lower the metal abundance, the smaller the luminosity drop during inflation. As the metallicity decreases below a critical value (function of mass), the ignition of helium in the core anticipates, and then suppresses the onset of the thermal instability (see Paper I). This is evident when comparing tracks referring to stars with the same mass but different metallicity, such as those displayed in Figure 15 in Iben & Renzini (1984), showing that 5 and 7 $M_\odot$ models with $Z = 0.001 \simeq Z_\odot/20$ ignite helium as a blue giant, and do not experience a runaway inflation until after the second blue loop: low-metallicity stars need a specially strong *kick* to become red giants.

And what happens to zero metal stars? Would a star be able to become a red giant even in absence of heavy metals? Could a radiative flow-trapping instability arise even in $Z = 0$ stars? Only few zero-metal models exist in the literature, and a systematic exploration remains to be done. The 10 $M_\odot$ models with $Z = 10^{-8}$ computed by Tornambè (1984) represent an excellent approximation to $Z = 0$ objects. These models spend all their lifetime in the blue and ignite carbon when their effective temperature is still in excess of 20,000 K. The same behavior is exhibited by the strictly $Z = 0$ models computed by Castellani, Chieffi, & Tornambè (1983). We note that the core of these models exceeds the Schönberg-Chandrasekhar limit, develop a μ gradient which is as large as that developed by metal-rich stars together with the associated local jump of polytropic index, and yet never become red giants. As noted in Paper I, reaching the Schönberg-Chandrasekhar limit, or developing a large μ gradient, or a large central concentration is not a sufficient condition for a star to become red giant. As also noted in the same paper, it is not even a necessary condition, as models of massive stars with fake opacity (Stothers & Chin 1977; Greggio 1984; Bertelli, Bressan, & Chiosi 1985) experience a runaway inflation to red giant dimensions while still burning hydrogen in their core, thus producing red giants with a main-sequence chemical structure. These considerations should suffice to invalidate another recent conjecture for the origin of the evolution to red giant structures, where Eggleton & Cannon (1991) attribute it to the development of a narrow region with effective polytropic index in excess of 5, which physically coincides with the shell across which μ drops by nearly a factor of 2. Instead, as emphasized in Paper I, the occurrence of the thermal instability leading to evolution to red giants cannot be unambiguously associated with any particular evolutionary stage, i.e., with any particular structure of the core. Most often it happens during the early shell hydrogen-burning stage, but it can be delayed to the double-shell burning stage if metallicity is sufficiently reduced, or even anticipated to the main-sequence phase if envelope opacity is sufficiently increased.[9] The lesson to draw from these considerations is that understanding the apparently erratic circumvolutions of stars in the H-R diagram requires us to focus at least as much attention on the physical processes taking place in the envelope, as one does on those taking place in the core. This attitude has been scarcely followed so far.

There remains to answer the question as to whether the presence of metals is instrumental to producing a runaway envelope expansion with negative W's, etc. The answer to this question is probably negative. The quoted 10 $M_\odot$ track by Tornambè exhibits indeed a negative W shortly before carbon ignition, signaling that radiative-flow trapping is at work, although the stellar explosion aborts its runaway inflation to red giant dimensions. What is probably going on is that the runaway expansion is driven by the recombination of hydrogen and, especially, helium in the envelope, with its effect on opacity and opacity derivatives. In this specific case carbon ignition may abort the attempt of the star to become a red giant, that shortly after will explode as a blue, Type II supernova. This suggests that zero-metal less massive stars which do not explode, but instead develop a degenerate carbon-oxygen core, may indeed experience a runaway expansion to red giants, as their luminosity increases by a much larger amount during the double-shell phase. In this case the instability would be driven by the helium and hydrogen opacity, as these elements start recombining in the envelope. Judging from their figure, the 5 $M_\odot$, $Z = 0$ model of Chieffi & Tornambè (1984) seems indeed to show a negative W just before reaching the Hayashi line as an AGB star.

Related to this issue is the numerical experiment performed by Weiss (1989) with a 15 $M_\odot$ model, in which a straight, constant opacity through the whole star was assumed. During its double-shell phase the model evolves towards the red giant region, but does so with increasing luminosity, i.e., W remains positive, and no thermal instability is encountered. The result is quite obvious indeed: in this case both α and β are zero, and

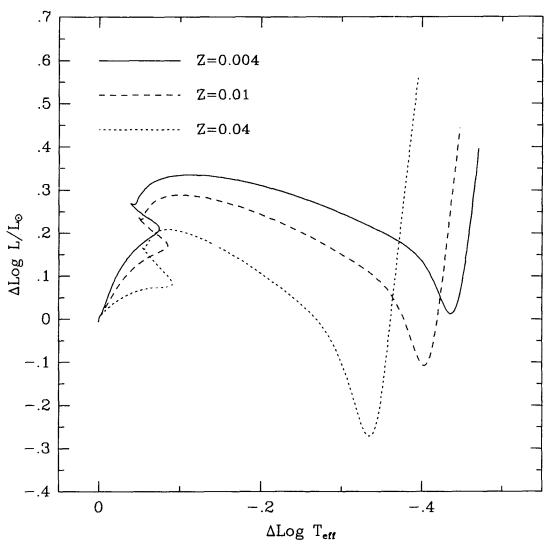

FIG. 23.—Evolutionary sequences up to core helium ignition for 3 $M_\odot$ stars of three metallicities, as indicated in the figure. The tracks are from Sweigart et al. (1989). The differences between log L and log $T_{\rm eff}$ and the corresponding ZAMS values are plotted.

[9] Although models exhibiting this latter type of behavior have been obtained with unphysical opacities, perhaps super metal-rich massive stars may evolve in this way, a possibility that could be easily tested by computing the corresponding sequences.

equation (9) indicates that a thermal instability is unlikely to arise. As far as the expansion is concerned, it clearly results from the ordinary secular increase of the core luminosity, which in the case of Weiss's experiment is substantially exaggerated by the resulting oversized helium core. With a pure electron-scattering opacity the GTHC would degenerate to a straight line with $L_S \simeq L_B$, provided L_B is not varied too rapidly.

5.4. *The Precursor of SN 1987A*

Although theoreticians had produced blue supergiant (BSG) exploders well in advance of the famous Magellanic Cloud display of 1987 February (e.g., Lamb, Iben, & Howard 1976; Maeder 1981; Brunish & Truran 1982; Castellani et al. 1983), most astronomers were much surprised by the event, and many claimed it was totally unexpected. However, apart from those of Maeder, these models spend their whole lifetime on the blue side of the H-R diagram, and it was soon realized (Renzini 1987a, b) that they are not applicable to the dominant population of LMC, which instead is rich with red supergiants (RSG) at the luminosity of Sk −60 202 (the precursor of SN 1987A). Therefore, Renzini argued that also Sk −69 202—if not an exceptional object in the LMC population—should have experienced a red supergiant phase before its final excursion to the blue, and that a possible check of the MS → BSG → RSG → BSG → SN evolutionary sequence would have been the detection of a light echo produced by the early optical and UV flash of the SN on the fossil RSG wind material.

Unlike the Lamb et al., Brunish & Truran, and Castellani et al. models. the models of Maeder (1981) do present a RSG phase before explosion, and therefore immediately looked more attractive. These models follow from earlier speculations according to which below a critical mass M_W stars terminate their evolution as RSGs and explode as (classical) Type II SNs, while above it the RSG wind is so effective as to strip most of the hydrogen-rich envelope thus forcing stars to evolve to the blue where they develop Wolf-Rayet characteristics, and eventually explode as some variety of Type I SNs (Renzini 1976, 1978; Maeder & Lequeux 1982). In the frame of this scenario Sk −69 202 would have been caught by core collapse and SN explosion just while rapidly sweeping across the H-R diagram in its final RSG to WR transition, a fairly rare event indeed. Now also this scenario can be excluded for the specific case of SN 1987A, as it would predict the presence of just a tiny amount of hydrogen at the stellar surface, less than $\sim 3\ M_\odot$ according to Maeder (1987), while the object exploded with still a substantial hydrogen envelope in place (Arnett et al. 1989). Also, the bulk of WR stars in LMC appear to originate from precursors more massive than $\sim 40\ M_\odot$ (Humphreys 1984), while the initial mass of Sk −69 202 was $\sim 20\ M_\odot$. Clearly, the final RSG to BSG transition was triggered by something else than an almost total stripping of the hydrogen envelope, i.e., by either the first or the second blue loop.

Evolution theory is in a great embarrassment in predicting the time Δt elapsed since the beginning of the final RSG-BSG transition, as a priori there exists a continuum of possibilities and too many parameters control the formation of blue loops. In this connection, it was soon noticed that the detection of light echoes would have been of great help in reconstructing the past evolutionary history of the precursor (Renzini 1987a, b). If present, the fossil RSG wind would lie at a distance from the exploding object given by

$$D \simeq 1 \text{ pc} \left(\frac{v_{\text{wind}}^{\text{RSG}}}{10 \text{ km s}^{-1}}\right)\left(\frac{\Delta t}{10^5 \text{ yr}}\right), \quad (14)$$

where $v_{\text{wind}}^{\text{RSG}}$ is the velocity of the RSG wind, and $\Delta t = \Delta t_{\text{tr}} + \Delta t_{\text{BSG}}$ clearly results from the sum of the duration of the RSG to BSG transition Δt_{tr}, plus the residual time spent as a BSG after this transition. While Δt_{tr} is of the order of the Kelvin-Helmholtz time scale for the envelope ($\sim 10^4$ yr), Δt_{BSG} depends instead on the precise phase at which the transition is initiated, and can in principle be anywhere from zero to almost the whole core helium-burning lifetime ($\sim 10^6$ yr). For example, in the 9 $M_\odot$ model presented in § 4, $\sim \frac{2}{5}$ of the core helium-burning lifetime are spent in the RSG phase, and the remaining $\frac{3}{5}$ in the BSG phase (see Fig. 21), but these ratios could be drastically changed by any of the subtle effects discussed in § 5.1. Of course, the same considerations hold also for the case of a $\sim 20\ M_\odot$ model.

It being so hard to predict Δt_{BSG}, a semiempirical approach is more effective, and from the fact that in the LMC there are roughly equal numbers of BSGs and RSGs one can estimate $\Delta t_{\text{BSG}} \simeq 5 \times 10^5$ yr, since $\Delta t_{\text{BSG}}/\Delta t_{\text{RSG}} \simeq 1$ and the whole helium-burning lifetime is $\sim 10^6$ yr. According to equation (14) this would imply that RSG wind material should have been found only at distances greater than ~ 5 pc from the SN, "*unless the story of Sk −69 202 was even more complicated, with a second RSG stage, and a final retreat to the blue triggered by one of the latest burning stages in the core ...*" (Renzini 1987b).

Exciting evidence has accumulated since these early speculations, and the presence of a fossil RSG wind is now well established. Narrow emission lines were soon detected in both the UV (Cassatella 1987; Kirshner et al. 1987; Fransson et al. 1989) and the optical (Wampler & Richichi 1988) and attributed to fluorescence emission from the fossil RSG wind, i.e., from what is now known as the celebrated circumstellar *ring* located at only 0.2 pc from SN 1987A (Jakobsen et al. 1991). So the final RSG-BSG transition did not take place in the middle of the core helium burning stage, but according to equation (14)—with $v_{\text{wind}}^{\text{RSG}} = 15$ km s^{-1} it took place only $\sim 13{,}000$ yr ago, i.e., just about one thermal time scale before explosion. Yet, this is not the whole story. Bond et al. (1989) have in fact detected an optical light echo on circumstellar dust, with the scattering material being located at some 5 pc from the supernova, which implies that Sk −69 202 was a RSG also more than 300,000 yr ago, when certainly it was still burning helium in the core.

Two evolutionary scenarios survive these evidences, that we call the single and the double RSG stage scenarios, respectively. In the former case the evolution proceeds following the sequence

$$\text{MS} \rightarrow \text{BSG} \rightarrow \text{RSG} \rightarrow \text{BSG} \rightarrow \text{SN},$$

with helium being ignited during the first BSG stage and exhausted during the subsequent RSG stage, as in the models of Woosley, Pinto, & Weaver (1988b); see also Figure 3 in Arnett et al. (1989). Here the first blue loop is therefore initiated in the blue. Alternatively, in the double-RSG scenario the evolution proceeds following the sequence

$$\text{MS} \rightarrow \text{BSG} \rightarrow \text{RSG} \rightarrow \text{BSG} \rightarrow \text{RSG} \rightarrow \text{BSG} \rightarrow \text{SN},$$

as speculated by Renzini (1987b), and actually performed by the models of, e.g., Langer (1991).

Whatever the real path followed by Sk −69 202, the question is: what interior event has triggered the final RSG-BSG transition? The fact that shortly after the transition the star exploded makes the answer to this question easier than one would have anticipated. Indeed, a transition during the core helium-burning phase is ruled out, since the whole duration of this phase is far too long ($\sim 10^6$ yr). The transition had to take place later, during a more advanced evolutionary stage. Past helium exhaustion in the core, the star spends $\sim 5 \times 10^4$ yr burning helium in a shell, then it takes only 300 yr to burn carbon, ~ 5 months to burn neon, ~ 6 months to burn oxygen, and finally 2 days to burn silicon (see Arnett et al. 1989). Clearly, the transition had to start during the shell helium-burning stage, more precisely at about $\frac{3}{4}$ of its duration. From the numerical experiments illustrated in § 3 we have learned that a RSG star on the Hayashi track initiates a blue excursion when the bottom luminosity L_B drops below a critical value. From § 4.7 we have also seen that during the shell helium-burning stage a drop of L_B is produced when the expansion front promoted by the helium-shell ignition comes through the hydrogen shell, thus switching it off, i.e., when the second blue loop is initiated. We conclude that *core collapse and explosion caught Sk −69 202 while it was performing its second blue loop.* Several corollaries follow from this conclusion. The first is that at the time of explosion the star was much away from TE. Indeed, shortly before the explosion TE was first broken by helium exhaustion in the core, which in the case of the double-RSG scenario was soon followed by the onset of the thermal instability in the envelope leading to the last BSG-RSG inflation. Further departure from TE was caused by helium ignition in the shell, while in the meantime the envelope reached the Hayashi line and was approaching its own TE when hydrogen-shell quenching caused a new departure from TE: an envelope instability soon developed leading to its runaway deflation. Departures from TE affected more and more the whole structure as carbon ignited in the core, the deep core included, although these departures developed on time scales much shorter then the Kelvin-Helmholtz time scale of the envelope. Correspondingly, the envelope did not have the time to react to these events in the deep interior. When, finally, on 1987 February 23 the core collapsed, the envelope was still responding to the hydrogen-shell quenching caused by the helium-shell ignition. The sequence of departures from TE is only marginally simpler in the case of the single-RSG scenario, as core helium exhaustion does not correspond to a BSG-RSG inflation, the star being already a RSG. The fact that during the last few 10^4 yr the star is intimately characterized by strong departures from TE makes excessively restrictive the approach of using static models to guess the configuration of the star at the moment of explosion (e.g., Saio, Kato, & Nomoto 1988; Tuchman & Wheeler 1989; Barkat & Wheeler 1990), as also pointed out by Arnett (1991).

Having recognized that Sk −69 202 was undergoing its second blue loop when the core collapsed, and therefore that the precursor was looping across the H-R diagram on a thermal time scale, it follows that any subtle effect able to anticipate or delay the last RSG-BSG transition (and in the double-RSG scenario also the last BSG-RSG transition) would have also dramatically affected the optical display of the supernova. In fact, any such effect would have influenced the precise phase along the second blue loop at which core collapse took place, and therefore the stellar radius which varies by a huge factor (~ 100) during the second blue loop. Correspondingly, it would have also affected the light curve of the supernova which is primarily determined by the stellar volume at explosion. We are therefore in the presence of a fantastic *amplifier*, such that small differences in apparently minor details can result in enormous differences in the supernova luminosity. For example, increasing a little bit the envelope opacity one would delay the RSG-BSG transition, and the explosion would catch the star at an earlier stage along its second blue loop, with the stellar radius being larger, the larger the opacity increase, or smaller depending on whether the explosion takes place before or after the turning point (point K in Fig. 1). Seemingly, reducing the Kelvin-Helmholtz time scale of the envelope (e.g., by stripping part of its mass) would accelerate the second blue loop, and the star might have the time to complete the loop before exploding, i.e., the star could return to the RSG branch (completing phase K-L, see Fig. 1) and would explode as a RSG. The situation is in part illustrated by some of the models available in the literature. For example, the model of Langer (1991) explodes near maximum temperature (minimum radius) along its second blue loop, i.e., close to point K (see Fig. 1). The model of Woosley et al. (1988b), instead, evolves slightly faster, and has the time to start its envelope inflation (a little past point K) before being striken by the explosion.

Certainty and indeterminacy mix in a subtle way in the case of SN 1987A. It is virtually certain that the precursor was running along its second blue loop at the time of explosion, but it will be virtually impossible to ascertain which specific combination of opacity, metallicity, mass loss, and convective mixing at the core boundary, above the hydrogen shell, and below the convective envelope, etc., was responsible for (1) the development of an extended second blue loop, and (2) for the particular position of the star along this loop when the core finally collapsed. Simply, in a multiparameter space like this, there are too many possible combinations which lead to the same final result, and it may be a waste of time trying to explore every possible combination. Yet, there is a point we would like to make here: the development of a second blue loop being so sensitive to input parameters, and so *casual* being the phase along this loop at which the star explodes, we can anticipate that right in the LMC, stars with slightly different mass, or slightly different metallicity, or slightly different rotationally induced mixing (if any), may well explode as RSG rather than BSG, and therefore exhibit a more canonical SN Type II luminosity evolution. Of course, these considerations are relevant for the question of the frequency in galaxies of underluminous supernovae, as SN 1987A was, but we postpone to a future paper the presentation of specific numerical examples; suffice here to emphasize that *every (non-WR) massive star explodes "in fly" as a second blue looper*, whatever the extension of the blue loop is.

One final question remains: did Sk −69 202 follow the single- or the double-RSG evolutionary path? Again, the possibility to distinguish between these a priori legitimate possibilities comes from the observation of the fossil RSG wind. In the former case the star would have been uninterruptly a RSG from several 10^5 yr to $\sim 10^4$ yr before the explosion, and correspondingly fairly dense, low-velocity material should now be present from ~ 0.2 pc to several pc from the supernova. In the latter case instead, low-velocity material should be absent in the distance range from ~ 02 pc to ~ 5 pc, corresponding to the BSG phase of the progenitor, i.e., there should be two separate circumstellar shells, corresponding to the first and the second RSG wind. According to their observations of SN

1987A light echoes, Crotts & Kunkel (1991) conclude that slow-moving material is present all the way from the inner ring at 0.2 pc to the outer shell discovered by Bond et al. at ~ 5 pc from the supernova. If so, one should inescapably conclude in favor of the single-RSG scenario, and correspondingly the models which would best reproduce the past evolution of Sk -69 202 would to be those of Woosley et al. (1988b) which ignite and burn helium in the red. However, these models fail to predict the observed blue to red supergiant ratio in LMC, which rather suggest that massive stars in LMC ignite helium in the blue, and spend as BSG a major fraction of their core helium-burning phase. We shall explore further these aspects in a future paper.

5.5. *Helium Giants*

Since the early work of Paczyński (1971; see also Iben & Tutukov 1985; Weiss 1987; Limongi & Tornambè 1991) it is known that helium star models in an appropriate mass range are able to cross the H-R diagram and to evolve to the giant region. Yet, these models do so with monotonically increasing luminosity, i.e., without the luminosity drop which is characteristic of runaway inflations in hydrogen-rich stars. This is probably due to the lower opacity of helium-rich envelopes (lower number of electrons per gram) which reach the Hayashi line before thermal instability has a chance to develop. We speculate that a true runaway inflation, with the associated luminosity drop, could be experienced also by helium envelopes provided the efficiency of convection is sufficiently reduced, for example by reducing the mixing length. If so, there would be no qualitative difference between hydrogen-rich and helium envelopes. A hint in this sense comes from the 2 $M_\odot$ helium star of Savonije & Takens (1976), which presents a small but noticeable decrease of luminosity in its way to the red giant region, signalling that radiative flux is being trapped in the envelope.

6. DISCUSSION

Having realized that stars become red giants in response to an increasing luminosity provided by the core which drives the envelope to run into a catastrophic decrease of radiative thermal conductivity, we also understand why those who searched the solution exploring the UV plane have failed to find the right answer (e.g., Yahil & van den Horn 1985; Fujimoto & Iben 1991). Indeed, the two homology invariants $U = 4\pi r^3 \rho / M_r$ and $V = GM_r \rho / rP$ (Chandrasekhar 1939) do not even contain either the trigger of the expansion (the luminosity), nor the cause of the thermal instability (the opacity), i.e., the relevant physics simply lies in others than the UV plane. For the connoisseur the UV plane can map the difference in the hydrostatic structure of a giant compared to a dwarf, but one will never find in the UV flatness the key as to why a dwarf inflates to become a giant.

Sometimes, starting with Lynden-Bell & Wood (1968), following an analogy with star clusters the transition to red giant structures has been associated with the *gravothermal catastrophe* of isothermal spheres. In this respect we note that the most rapid contraction of the stellar core takes place during the overall contraction phase, when rather than expanding to red giant dimensions the envelope actually contracts. Therefore, the analogy with the gravothermal catastrophe of a cluster is physically invalid because crucial to the physical phenomenon of stellar inflation is the fact that a radiative energy flux has to be carried out and radiated away. Radiative losses are instead irrelevant for the dynamical evolution of a cluster, which is an isolated system, while the star is not.

Applegate (1988) argues that there exists a maximum luminosity that a radiative envelope can transmit, and that the star is forced across the Hertzsprung gap to the red giant branch when this luminosity is exceeded. This statement looks correct if one considers the evolution around point D in Figure 1, but the argument does not have general validity. Indeed, during the core helium-burning phase (from point H to point I) the luminosity exceeds that of the local maximum at point D, the envelope is radiative, and not only is it in almost strict TE but it is even contracting rather than expanding. Another counterexample is provided by the GTHC in Figure 2. Clearly, the structure of the envelope is not uniquely determined by the luminosity, but it also depends on its previous history. In essence, the maximum luminosity criterion applies to expanding, not to contracting, envelopes. A contracting envelope in radiative equilibrium can in fact keep brightening according to the $L \propto R^{-1/2}$ law, and every luminosity could be exceeded without the star becoming a red giant, were it not for other effects.

All of us belong to a generation which has little familiarity with the debates on stellar structure and evolution preceding the mid-sixties. Since then computers allowed the *creation* of extremely detailed and physically accurate models, and—to tell the truth—we all have just ignored the pioneering works of the classics, Eddington, Jeans, and Chandrasekhar. The scope of this paper is not at all historical, and we do not attempt at answering the question why it took so long to understand "why stars become red giants." But eventually we had a cursory look at the treatises of Eddington (1926), Jeans (1928), and Chandrasekhar (1939).

We have not been able to find anything related to our problem in the treatise of Chandrasekhar, while Eddington addresses the question of stellar stability only in his § 211, where he argues that the generation of nuclear energy must depend on density and temperature. For, if L_N were independent of R a radiative star in which $L_S \propto R^{-1/2}$ would contract indefinitely as a deficit $L_S - L_N$ would become worse as the star contracts. For this reason Eddington correctly believed that stellar energy was generated by nuclear reactions between free particles. But in his treatise he does not explicitly give or discuss a general criterion for stellar stability.

Jeans believed that stars were *liquid* spheres, taking their energy from the annihilation of protons with electrons. He also thought that only bound electrons could annihilate with protons in atomic nuclei, and not—in case—because their wave function within nuclei is larger than for free electrons, but because—contrary to Eddington—he wanted the coefficient of nuclear energy generation to be almost independent of temperature and density. Otherwise, he claimed, stars "would be unstable through a tendency to develop explosive pulsations." He was clearly wrong, and following this reasoning Jeans concluded that stars ought to be made up mostly of transuranic elements, so as to ensure the presence of bound electrons—and so nuclear energy generation—at the high temperatures found in stellar interiors. His condition for stellar stability was, in modern notations (see his eq. [144.2]):

$$\frac{\delta \ln L_S}{\delta \ln R} > \frac{\delta \ln L_N}{\delta \ln R} . \tag{15}$$

Jeans called this inequality the condition for *dynamical* stability, but in reality even when it is violated the star does not

encounter any difficulty in maintaining its hydrostatic equilibrium, i.e., contrary to Jeans' belief the star does not explode. Note that equation (15) refers to the whole star, while, following Ledoux (1958), Kippenhahn & Weigert (1990) insist instead for a vaguely similar condition to hold *locally* for the generic mass shell, and call it the conditions for *secular* stability. It certainly takes many centuries for the instability to develop when inequality (15) is violated, but we find that also this terminology is inappropriate to specify the kind of instability described by this inequality. Indeed, when (15) is violated, it is the *thermal* equilibrium which is broken, and therefore (15) is the condition for *thermal stability*. Moreover, the weakness of the core-envelope coupling during the advanced evolutionary stages that we have illustrated in § 4, makes it also clear that a condition for thermal stability cannot be merely local. Indeed, Ledoux (1958) and Kippenhahn & Weigert (1990) translate the condition for what they call the secular stability into an inequality connecting the *local* temperature and density derivatives of $\epsilon_n \propto \rho^a T^b$ and $\kappa \propto \rho^\alpha T^{-\beta}$, see their equations (14.35) and (25.37), respectively. The condition they derive is, with our notations,

$$3a + b > \beta - 3\alpha \,. \tag{16}$$

In practice, this relation follows from asking the variation in the luminosity transmitted by a generic shell to be balanced by a variation of nuclear energy generated within the shell itself. As such, the criterion ignores the occurrence of evolutionary variations of L_r which are not compensated locally, but which can or cannot be compensated by variations of L_N, wheresoever L_N is generated. Conversely, it is easy to realize that the stability condition (16) is never violated, *even when the envelope is thermally unstable*! Indeed, $a = 1$, and 2, respectively, for hydrogen and helium burning, and $b \simeq 4$, 15, and > 30, respectively, for the *pp*-chain, the CNO cycle, and the 3α-process, and so the left-hand side of this inequality ranges from ~ 7 to over ~ 36, while the right-hand side is at most ~ 0.5, when Kramers opacity applies. Since condition (16) is never violated it does not say anything; in particular it does not say when the envelope becomes thermally unstable. It follows that the local criterion of Ledoux (1958) and Kippenhahn & Weigert (1990) should be abandoned, while only a nonlocal, global criterion can incorporate the delicate feedback between envelope expansion/contraction and the strength of the burning shell.[10] We have formulated this criterion for thermal stability in § 4.4., and it is easy to realize that equation (15) is nothing else than equation (13) when written for the whole star, i.e., for $M_r = M$ and $r = R$. So Jeans was right after all! He had wrong ideas about stellar composition, equation of state, and nuclear energy generation, and perhaps for this reason his correct criterion for "*dynamic*," "*secular*," actually *thermal* stability has been forgotten. To our knowledge, nobody has ever associated equation (15) to the formation of red giants and blue loops, and yet right there is the explanation of both phenomena.

7. CONCLUSIONS

The main results presented in this paper can be summarized as follows:

1. We have demonstrated that stars become red giants in response to the increasing luminosity being provided by the stellar core, and that the runaway expansion—when it takes place—is triggered by the thermal conductivity in the envelope reaching a maximum and then decreasing. The decrease of thermal conductivity is caused by the opacity increase promoted by the recombination of heavy ions in the envelope, as the envelope itself expands and cools.

2. We have shown that the decrease in thermal conductivity at each point in the envelope causes part of the radiative energy flow to be trapped locally, which causes further expansion and further departure from thermal equilibrium. When this happens it is a thermal instability in the envelope to cause the inflation to the red giant region. The onset of the thermal instability is macroscopically signaled by the stellar luminosity being decreased during expansion, a condition which suffices to identify all runaway inflation episodes taking place in the course of evolution.

3. Thermal equilibrium in the stellar envelope is restored by the onset of convection, as the star approaches the Hayashi line. The thermal instability being produced by a trapping of the radiative energy flow, the instability itself is quenched when the mode of energy transfer turns from radiative to convective.

4. As expansion to red giants is driven by the evolutionary *increase* of the input luminosity at the base of the envelope, so during the core helium-burning phase the evolutionary *decrease* of such luminosity drives the same kind of instability to work in the *reverse* direction: as the inner envelope returns radiative contraction favors further energy losses in a runaway deflation which leads to the formation of the so-called first blue loop.

5. The second blue loops are produced by the rapid drop and subsequent rapid increase of the input luminosity at the base of the envelope, associated to the extinguishment of the hydrogen-burning shell and the subsequent leakage from the core to the envelope of the energy released by the just ignited helium-burning shell. During the whole second blue loop stars are far away from thermal equilibrium.

6. It is recognized that every runaway contraction from the Hayashi line that can take place in the course of evolution is basically due to the same physical process leading to the formation of blue loops. This is in particular the case for the initial contraction from the Hayashi line to the zero-age main sequence.

7. A general criterion for thermal stability is formulated (eq. [13]), and it is shown that when it is violated the envelope undergoes either runaway expansions to, or runaway deflations from red giant dimensions, depending on the previous evolution.

8. The runaway deflation leading to the formation of blue loops being triggered by the luminosity at the base of the envelope decreasing below a threshold value, the role of various model ingredients on the formation and extension of blue loops is analyzed and clarified by looking at their effect on the approach of such luminosity to the critical threshold. Such model ingredients include overshooting from convective cores and envelopes, mass loss, semiconvection, stellar mass, metallicity, and reaction rates.

9. It is demonstrated that the precursor SN 1987A, i.e., the star Sk −69 202, was describing its second blue loop in response to the hydrogen-shell extinguishment when its core collapsed and the object exploded. It is argued that very small mass and metallicity differences may suffice to significantly accelerate or decelerate the rate with which the second blue loop is percurred, thereby significantly affecting the stellar

[10] It is easy to realize that also the *nonlocal* criterion offered by Ledoux (1958, his eq. [14.38]) fails to predict the existence of thermal instabilities, and therefore it is invalid. As a further example, we note that in the case of a thermonuclear flash—such as the core flash or helium-shell flashes—condition (16) is verified in the flashing region, and yet the star departs most dramaticaly from TE.

radius at explosion, and having a macroscopic impact on the luminosity and luminosity evolution of the supernova.

10. It is finally argued that the use of homology invariants cannot significantly help to understand the physical origin of runaway inflations and deflations, and that the existence of μ gradients, rapid core contractions, and polytropic index variations—occasionally blamed for the expansion to red giant dimensions—do not have a direct role on such transformation. It is shown instead that a forgotten criterion that Jeans (1925, 1928) intended for the stellar *dynamical* stability, actually describes the condition for the stellar *thermal* stability that we have generalized in this paper, and applied to explain red giant as well as blue loop formation.

We are most indebted to Icko Iben Jr. for having kindly provided to us his stellar evolution code "FUJIMO" that we have extensively used to prove our explanation of red giant and blue loop formation mechanism. His code proved to be the least affected by *numerical microquakes* which can otherwise add disturbing noise when computing the evolutionary derivatives such as the W function. We only regret that—being absorbed in other projects—it took us seven years to make good use of such a flexible and powerful tool. We are also indebted to Sandro Chieffi for having computed for us in 1982 an evolutionary sequence of a 5 $M_\odot$ star that was used for a first check of the idea. A. R. also acknowledges Dave Arnett, Zalman Barkat, Icko Iben Jr., Craig Wheeler, and Amos Yahil for the stimulating debate on this issue that took place at the 1984 Summer Institute in Aspen. Achim Weiss is acknowledged for having kindly provided a preprint of his 1989 paper in advance of publication. Finally, we are indebted to Arlin Crotts for having drawn our attention on his light echo observations which allow to disentangle between the single- and the double-RSG scenario for the pre-supernova evolution of SN 1987A. This research has been supported in part by the Italian Ministry of Research (MURST) via "40%" and "60%" grants.

REFERENCES

Alongi, M., Bertelli, G., Bressan, A., & Chiosi, C. 1991, A&A, 244, 95
Applegate, J. H. 1988, ApJ, 329, 803
Arnett, W. D. 1991, ApJ, 383, 295
Arnett, W. D., Bahcall, J. N., Kirshner, R. P., & Woosley, S. E. 1989, ARA&A, 27, 629
Barkat, Z., & Wheeler, J. C. 1990, ApJ, 341, 925
Becker, S. A. 1981, ApJ, 248, 298
Becker, S. A., Iben, I., Jr., & Tuggle, R. S. 1977, ApJ, 218, 633
Bertelli, G., Bressan, A. G., & Chiosi, C. 1985, A&A, 150, 33
Bhaskar, R., & Nigam, A. 1991, ApJ, 327, 592
Bond, H. E., Gilmozzi, R., Meakes, M. G., & Panagia, N. 1989, ApJ, 354, L49
Brunish, W. M., & Becker, S. A. 1990, ApJ, 351, 258
Brunish, W. M., & Truran, J. W. 1982, ApJS, 49, 447
Cassatella, A. 1987, in ESO Workshop on the SN 1987A, ed. I. J. Danziger (Garching: ESO), 101
Castellani, V., Chieffi, A., & Tornambè, A. 1983, ApJ, 272, 249
Castellani, V., Giannone, P., & Renzini, A. 1971, Ap&SS, 10, 355
Chandrasekhar, S. 1939, An Introduction to the Study of Stellar Structure, edition 1957 (NY: Dover)
Chieffi, A., & Tornambè, A. 1984, ApJ, 287, 745
Chiosi, C. 1990, in Confrontation Between Stellar Pulsation and Evolution, ed. C. Cacciari & G. Clementini (ASP Conf. Ser., 11), 158
Chiosi, C., Bertelli, G., & Bressan, A. G. 1992, ARA&A, in press
Crotts, A. P. S., & Kunkel, W. E., 1991, ApJ, 366, L73
Eddington, A. S. 1926, The Internal Constitution of Stars, ed. 1959 (NY: Dover)
Eggleton, P. P., & Cannon, R. C. 1991, ApJ, 383, 757
Eggleton, P. P., & Faulkner, J. 1981, in Physical Processes in Red Giants, ed. I. Iben Jr. & A. Renzini (Dordrecht: Reidel), 179
Fransson, C., et al. 1989, ApJ, 336, 429
Fujimoto, M. Y., & Iben, I., Jr. 1991, ApJ, 374, 631
Greggio, L. 1984, in Stellar Nucleosynthesis, ed. C. Chiosi & A. Renzini (Dordrecht: Reidel), 137
Henyey, L. G., LeLevier, R., & Levée, R. D. 1955, PASP, 67, 154
Humphreys, R. M. 1984, in Observational Tests of the Stellar Evolution Theory, ed. A. Maeder & A. Renzini (Dordrecht: Reidel), 279
Iben, I., Jr. 1965a, ApJ, 141, 993
———. 1965b, ApJ, 142, 1447
———. 1967, ARA&A, 5, 571
Iben, I., Jr., & Renzini, A. 1984, Phys. Rep., 105, 329
Iben, I., Jr., & Tutukov, A. V. 1985, ApJS, 58, 661
Jakobsen, P., et al. 1991, ApJ, 369, L63
Jeans, J. H. 1925, MNRAS, 85, 916
———. 1928, Astronomy and Cosmogony, edition 1961 (NY: Dover)
Kähler, H. 1978, in The HR Diagram, ed. A. G. D. Philip (Dordrecht: Reidel), 303
Kippenhahn, R., & Weigert, A. 1990, Stellar Structure and Evolution (Berlin: Springer)
Kirshner, R. P., et al. 1987, IAU Circ. No. 4435
Lamb, S. A., Iben, I., Jr., & Howard, W. M. 1976, ApJ, 207, 209
Langer, N. 1991, in SN 1987A and Other Supernovae, ed. I. J. Danziger & K. Kjär (Garching: ESO), 15
Lauteborn, D., Refsdal, S., & Weigert, A. 1971, A&A, 13, 119
Ledoux, P. 1958, in Handbuch der Physik, Band LI, ed. S. Flügge (Berlin: Springer), 605
Limongi, M., & Tornambè, A. 1991, ApJ, 371, 317
Lynden-Bell, D., & Wood, R. 1968, MNRAS, 138, 495
Matraka, B., Wassermann, C., & Weigert, A. 1982, A&A, 107, 283
Maeder, A. 1981, A&A, 102, 401
———. 1987, in WSO Workshop on the SN 1987a, ed. I. J. Danziger (Garching: ESO), 251
Maeder, A., & Lequeux, J. 1982, A&A, 114, 409
Maeder, A., & Meynet, G. 1989, A&A, 210, 155
Paczyński, B. 1971, Acta Astron., 21, 1
Podsiadlowski, Ph., Joss, P. C., & Hsu, J. J. L. 1992, ApJ, 391, 246
Renzini, A. 1976, in The Galaxy and the Local Group (RGO Bull. No. 182), 87
———. 1977, in Advanced Stages in Stellar Evolution, ed. P. Bouvier & A. Maeder (Geneva: Geneva Observatory), 149
———. 1978, Mem. Soc. Astron. Ital., 49, 389
———. 1984, in Observational Tests of the Stellar Evolution Theory, ed. A. Maeder & A. Renzini (Dordrecht: Reidel), 21 (Paper I)
———. 1987a, in Nuclear Astrophysics, ed. W. Hillebrandt, R. Kuhfuss, E. Müller, & J. W. Truran (Berlin: Springer), 305
———. 1987b, in ESO Workshop on the SN 1987A, ed. I. J. Danziger (Garching: ESO), 295
Renzini, A., & Fusi Pecci, F. 1988, ARA&A, 26, 199
Saio, H., Kato, M., & Nomoto, K. 1988, ApJ, 331, 388
Savonije, G. J., & Takens, R. J. 1976, A&A, 47, 231
Schwarzschild, M. 1958, Structure and Evolution of the Stars (NY: Dover)
Stothers, R., & Chin, C. W. 1977, ApJ, 211, 189
———. 1991, ApJ, 374, 288
Sweigart, A. V., Greggio, L., & Renzini, A. 1989, ApJS, 69, 471
———. 1990, ApJ, 364, 527
Taylor, R. J. 1988, Nature, 335, 14
Tornambè, A. 1984, MNRAS, 206, 867
Tuchman, Y., & Wheeler, J. C. 1989, ApJ, 346, 417
Wampler, E. J., Richichi, A. 1988, Messenger, 52, 14
Weiss, A. 1987, A&A, 185, 165
———. 1989, A&A, 209, 135
Whitworth, A. P. 1989, MNRAS, 236, 505
Woosley, S. E., Pinto, P. A., & Ensman, L. M. 1988a, ApJ, 324, 466
Woosley, S. E., Pinto, P. A., & Weaver 1988b, Proc. Astron. Soc. Australia, 7, 355
Yahil, A., & van den Horn, L. 1985, 296, 554